

**LINEAR ACCELERATOR MULTILEAF COLLIMATOR
QUALITY CONTROL METHODOLOGIES
IN RADIOTHERAPY**



Ayron Edward Rule

A Dissertation submitted to the Faculty of Science, University of the Witwatersrand, Johannesburg, in fulfilment of the requirements for the degree of Master of Science.

May 2016

DECLARATION

I declare that "Linear Accelerator Multileaf Collimator Quality Control Methodologies in Radiotherapy" thesis is my own work and that all sources that I have used or quoted have been indicated and acknowledged by means of complete references. It is being submitted for the Degree of Master of Science at the University of the Witwatersrand, Johannesburg. It has not been submitted before for any degree or examination at any other University.

(Signature of candidate)

30 day of May 2016

ABSTRACT

Introduction: The Multileaf collimator (MLC) system introduction into Clinical Linear Accelerators (Linacs), facilitated computer-control and verification of complex treatment, and results in an increase in patient set up speed. An MLC system thus requires a re-evaluation of the quality assurance (QA) requirements for beam collimation. This study investigated, developed, performed and evaluated QA efforts for conventional MLCs with the aim to evaluate the efficacy and reproducibility of the quality control (QC) procedures with different detectors.

Materials and Methods: The performance of MLCs for an Elekta (Livingstone Hospital) and Siemens (Charlotte Maxeke Johannesburg Academic Hospital) Linac were examined. The major QC procedures studied were leaf matching, leaf position accuracy, intraleaf leakage and transmission through abutting leaves. Three portal imaging devices (radiographic film, radiochromic film and an Electronic Portal Imaging Device) and a PTW LA48 Linear array were used as detectors. Record and verify data management systems were used to set up and execute the procedures. The calibration of all the portal imaging devices was also performed.

Results: The calibration procedure of the portal imaging devices is Linac specific in execution. The profiles obtained indicated consistency across device and time. A combined single execution procedure is viable and reproducible on all platforms.

Conclusion: The results show that the calibration of imaging devices is of great importance. The MLC design influences the range and extent of QC that can be performed. This may impact on the accuracy with which advanced technologies requiring high conformity and reproducible leaf movement, can be delivered. Imaging devices each have specific resource requirement issues affecting the efficacy of their use.

DEDICATION

To my family, my wife Nadia, my son Kayne and my daughter Mia, you are why and who I am and the reason I do what I do.

In memory of Dr Iona Ismail-Wesso, you will always be remembered and cherished.

ACKNOWLEDGEMENTS

This research report would not have been possible without the assistance and cooperation of certain individuals and institutions, and the author would particularly like to thank the following:

- My supervisor Professor D. G. van der Merwe for assisting me in choosing this topic, making the opportunity available to me and assisting me whenever and however I needed throughout the process.
- The departments of Radiation Oncology at Charlotte Maxeke Johannesburg Academic Hospital and Livingstone Hospital for allowing me to use their Linear accelerators.
- My colleagues, Ms Leandi van der Merwe and Mr Johan Engelbrecht for numerous discussions about the subject.
- My mother, Dr Iona Ismail-Wesso for your guidance and complete understanding.
- My wife, Nadia Wesso-Rule for your support, grammatical and overall writing assistance.

TABLE OF CONTENTS

CONTENTS	PAGE
DECLARATION	ii
ABSTRACT	iii
DEDICATION	iv
ACKNOWLEDGEMENTS	v
LIST OF FIGURES	ix
LIST OF TABLES	xv
ABBREVIATIONS	xvi
1. INTRODUCTION AND AIM	1
2. LITERATURE REVIEW	4
3. MATERIALS	9
3.1. Multileaf Collimators	9
3.2. Megavoltage 2 Dimensional Detectors	10
3.3. Ionization Chambers	11
3.4. Phantoms	11
3.5. Film Scanners and Dosimetric Software	12
4. METHODOLOGY	14
4.1. Experimental Test Procedures Introduction	14

4.2. Quality Control Test Procedures Design	14
4.2.1. Leaf matching test procedure	14
4.2.2. Leaf position accuracy test procedure	15
4.2.3. Intraleaf leakage and abuttal test procedures	16
4.2.4. Combined test procedure	19
4.3. Megavoltage 2 Dimensional Detectors and Linear Array Setup and Calibration	19
4.3.1. Radiographic film	20
4.3.2. Radiochromic film	23
4.3.3. Electronic Portal Imaging Device (EPID)	24
4.3.4. Linear array	24
5. RESULTS	26
5.1. Results of the MLC Performance at CMJAH	26
5.1.1. Calibration curves	26
5.1.2. Quality Assurance test procedure results	28
5.2. Results of the MLC Performance at LH	35
5.2.1. Calibration curves	35
5.2.2. Quality Assurance test procedure results	37
5.3. CMJAH and LH Results Comparison	45
5.3.1. Leaf matching test procedure	45
5.3.2. Leaf position accuracy test procedure	45
5.3.3. Intraleaf leakage and abuttal test procedures	46
5.3.4. Combined test procedure	46
5.4. Portal Imaging Device and Linear Array Observations	47
5.4.1. Processing and Analysis Assessment of Imaging Devices	48

6. ANALYSIS	50
6.1. Introduction	50
6.2. Leaf Matching Test Procedure Analysis	50
6.3. Leaf Position Accuracy Test Procedure Analysis	54
6.4. Intraleaf Leakage Test Procedure Analysis	58
6.5. Abuttal Test Procedure Analysis	60
6.6. Summary	60
7. CONCLUSION AND RECOMMENDATIONS	62
8. REFERENCES	64
APPENDIX	
Similarity Summary Report	68

LIST OF FIGURES

Figure 3.1:	Diagram of Elekta Linac jaw and leaf orientation in the Linac collimator head as used at LH. (Image found in Jordan <i>et al.</i> ¹⁶)	9
Figure 3.2:	Diagram of Siemens Linac jaw and leaf orientation in the Linac collimator head as used at CMJAH.	10
Figure 3.3:	Universal IMRT phantom structure indicating the film prickers, the chamber slots and the two sections of the phantom	12
Figure 4.1:	Diagram of leaf matching test procedure.	15
Figure 4.2:	Diagram of leaf position accuracy test procedure predicted result for the comparison between CMJAH and LH in this study.	16
Figure 4.3:	Diagram of the Elekta and Siemens MLC systems indicating the tongue and groove leaf configuration (Image found in Huq <i>et. al</i> ²⁴).	17
Figure 4.4:	Diagram of intraleaf leakage and abuttal test procedures for CMJAH. The thicker grey horizontal area indicates open leaves.	18
Figure 4.5:	Diagram of the intraleaf leakage test procedure for LH. The thicker grey horizontal area indicates open leaves.	18
Figure 4.6:	Diagram of the combined test procedure consisting of segments for leaf matching, leaf position accuracy, intraleaf leakage and abuttal test procedures.	19
Figure 4.7:	The positioning of the UIP for the exposure of films at the isocentre of the CMJAH Linac.	20
Figure 4.8:	The positioning of the UIP for the exposure of films at the SSD 63 cm setup for the CMJAH Linac.	21
Figure 4.9:	The positioning of the Polystyrene phantom for exposure of films at the isocentre of the LH Linac	21
Figure 4.10:	The positioning of the Polystyrene phantom for the exposure of the films at the SSD 63 cm setup for LH Linac.	22
Figure 4.11:	The position of the EPID for the exposure of EPID images for the LH Linac.	24
Figure 4.12:	The PTW MP3 water tank, support table and reservoir tank used with the LA 48 at CMJAH.	25
Figure 4.13:	The LA 48 set up in PTW MP-3 water tank for the CMJAH Linac	25

- Figure 5.1: Image (a) illustrates the Kodak X-Omat VTM film exposed at CMJAH to a 20 x 20 cm² field size at isocentre in the UIP phantom with 20 MU and a virtual wedge angle of 60⁰ for the purpose of calibration of the the Kodak X-Omat VTM film. Graph (b) is the linear-logarithmic curve obtained when plotting the measured optical density against the known dose for the corresponding MU field. 27
- Figure 5.2: The Gafchromic EBT2 calibration curve for CMJAH 6 MV photon beam. 27
- Figure 5.3: The calibration curve from the PTW LA48 Linear array obtained from a 20 x 20 cm² 60⁰ virtual wedge field delivered over 50 MU to the central axis. The curve was measured at a depth of 5.5 cm in water at isocentre. 28
- Figure 5.4: Image (a) is the Kodak X-OMat V film of the completed leaf matching test procedure obtained using the UIP phantom at 5cm depth in phantom with the film set up with a SSD of 63 cm for a 6 MV photon beam and 30 MU delivered per field segment. Graph (b) is the profile of the central X-axis as indicated on image (a). The data were obtained using the film calibration data, the MEPHYSTO software and adjusted to represent the field dimensions at isocentre. 29
- Figure 5.5: A comparison of the profile of the central X-axis produced from the Kodak X-OMat V film on the 22 September 2014 and the 03 April 2015. 29
- Figure 5.6: Image (a) is the Gafchromic EBT2 film of the completed leaf position accuracy test procedure obtained using the UIP phantom with the film set up with a SSD of 63 cm for 6 MV photon beam and 80 MU per field segment. Graph (b) is the profile of the field defined by the MLC along the central field segment as indicated on image (a). The data were obtained using the film calibration data, the MEPHYSTO software and adjusted to show the field dimensions as defined at isocentre. 30
- Figure 5.7: A comparison of the profile 1 cm along the Y-axis produced from the Gafchromic EBT2 film on the 21 September 2014 and the 03 April 2015. 31
- Figure 5.8: The LA 48 Linear array profile of Leaf 10 (5 cm from the central axis) to obtain the intraleaf leakage and perform the abuttal test procedure. A

- 2 mm step size was used with the LA 48 positioned at 5.5 cm depth in water at isocentre. 31
- Figure 5.9: The LA 48 Linear array profile measured parallel to the Y axis and 5 cm offset from the central axis with a 2 mm resolution. The LA48 was positioned at 5.5 cm depth in water at isocentre. 32
- Figure 5.10: Image (a) is the Kodak X-OMat V film of the completed combined test procedure obtained using the UIP phantom with the film at isocentre with 30 MU per field segment. Graph (b) is the profile along the central X-axis for leaf matching analysis, graph (c) is the Y profile at 6.5 cm from the central axis for intraleaf leakage analysis, graph (d) is the profile of leaf 7 in the MLC for abuttal analysis and graph (e) is the profile 1 cm off the Y axis for leaf position accuracy analysis. These are all indicated on image (a) and the data were processed using the film calibration data and the MEPHYSTO software package. 33-34
- Figure 5.11: A comparison of the profile of the central X-axis produced from the Kodak X-OMat V film on the 22 September 2014 and the 03 April 2015. 34
- Figure 5.12: Image (a) is one of the sets of the Gafchromic EBT2 calibration films for LH 8 MV photon beam obtained by cutting the Gafchromic EBT2 into 9 x 10 cm² pieces and exposing to increasing MU. Graph (b) is the linear-logarithmic curve obtained when plotting the measured optical density against the known dose for the corresponding MU field. 35
- Figure 5.13: Kodak X-OMat V calibration curve for LH 8 MV photon beam obtained by plotting known dose points on calibration films to measured optical density at the same points on the scanned film on a linear-logarithmic scale. 36
- Figure 5.14: A comparison of the leaf position accuracy test procedure along the X-axis profile obtained with Gafchromic EBT2 and Kodak X-OMat V films. 36
- Figure 5.15: Image (a) is a sample of the images used to generate the EPID dose response for the LH 8 MV photon beam. Graph (b) is the EPID dose response curve obtained 37
- Figure 5.16: Image (a) is the Kodak X-OMat V film of the completed leaf matching

test procedure (without back up jaws) in a field obtained using a polystyrene phantom. The film was placed at 5 cm depth in the phantom with an SSD of 63 cm and 30 MU per field segment was delivered. Graph (b) is the profile of the central X-axis as indicated on image (a). The data were obtained using the film calibration data, the MEPHYSTO software and adjusted to the field dimensions at isocentre. 38

Figure 5.17: A comparison of the profile without the back-up jaw in the field along the central X-axis produced from the Kodak X-OMat V film on the 16 November 2014 and the 13 March 2015. 38

Figure 5.18: A comparison of the profile with the back-up jaw in the field along the central X-axis produced from the Kodak X-OMat V film on the 16 November 2014 and the 13 March 2015. 39

Figure 5.19: Image (a) is the Gafchromic EBT2 film of the completed leaf position accuracy test procedure obtained using a depth of 5 cm in a 7 cm thick polystyrene phantom with the film at isocentre using 80 MU per field segment. Graph (b) is the profile of the edge of the field defined by the MLC for the central field segment as indicated on image (a) obtained using the calibration film data and the MEPHYSTO software. 40

Figure 5.20: A comparison of the profile 1 cm off the Y-axis produced from the Gafchromic® EBT2 film on the 11 November 2014 and the 13 March 2015. 41

Figure 5.21: The three EPID images required to produce the intraleaf leakage test procedure. 41

Figure 5.22: The EPID profile of 5 cm along Y-axis for the intraleaf leakage and abuttal test procedure. The central peak is from leaf 20 being open during the exposure. 42

Figure 5.23: Comparison of the intraleaf leakage profile for the EPID taken at two different times 42

Figure 5.24: Image (a) is the Kodak X-OMat V film of the completed combined test procedure obtained at 5 cm depth in a 7 cm thick polystyrene phantom at isocentre with each segment delivering 30 MU. Graph (b) is the profile of the central X-axis representing the leaf matching test procedure. Graph (c) is the profile of 6.5 cm off the Y-axis representing

	the intraleaf leakage test procedure and graph (d) is 1 cm off the Y-axis for performing the leaf position accuracy test procedure. The profiles are indicated in image (a) and the analysis was obtained using the film calibration data and the MEPHYSTO software package.	43
Figure 5.25:	A comparison of the profile of the central X-axis produced from the Kodak X-OMat V film on the 16 November and the 18 March 2015 with 100% defined as maximum value for each profile.	44
Figure 5.26:	The comparison of the leaf matching test procedure at CMJAH and LH using Kodak X-OMat V film.	45
Figure 5.27:	The comparison of the leaf position accuracy test procedure for CMJAH and LH exposed on Gafchromic EBT2 film.	45
Figure 5.28:	The comparison of the intraleaf leakage test procedure result from the LA 48 linear array (in water) at CMJAH and the EPID at LH (in air).	46
Figure 5.29:	The comparison of the combined test procedure for CMJAH and LH exposed on Kodak X-OMat V film.	47
Figure 5.30:	The comparison of the leaf matching test procedure for the portal imaging devices (Kodak X-OMat V and Gafchromic EBT2 films) and the LA48 linear array used at CMJAH.	47
Figure 5.31:	The comparison of the combined test procedure X-axis profile for the portal imaging devices (Kodak X-OMat V, Gafchromic EBT2 films and EPID) used at LH.	48
Figure 6.1:	An example of a leaf matching test procedure subfield with the position of the backup jaw and MLC shown with respected to the irradiated field size.	51
Figure 6.2:	An example of the method used to determine the FWHM values for the matching data results. The curve shown is for the LA 48 detector at position 100 mm from CAX.	52
Figure 6.3:	The leaf matching test procedure profiles for Kodak 2 and Gafchromic 2 showing the difference in the shape of the spikes at the matching positions.	53
Figure 6.4:	An example of the leaf position accuracy test procedure results for all imaging devices at CMJAH taken in September 2014 normalised to leaf 21 with leaves below 100% being out of the field and leaves above	

100% being in the field. 55

Figure 6.5: An example of the combined test procedure results for leaf position accuracy for Kodak and Gafchromic film at LH taken in March 2015 normalised to leaf 20 with leaves below 100% being out of the field and leaves above 100% being in the field. 55

LIST OF TABLES

Table 5.1:	The imaging devices used ranked from the shortest average exposure time needed on the Linac to obtain the test procedure results	48
Table 6.1:	Tolerance values according to AAPM TG 142 and CPQR 2013 for the test procedures conducted on the CMJAH and LH Linac systems.	50
Table 6.2:	The average FWHM for all leaf matching and combined test procedures for both CMJAH and LH for all imaging devices.	52
Table 6.3:	The average leaf position for all leaf position accuracy and combined test procedures for both CMJAH and LH for all imaging devices.	56
Table 6.4:	The deviation from 100% for CMJAH and LH for all leaf position accuracy and combined test procedures for all imaging devices where 100% corresponds to leaf 21 at CMJAH and leaf 20 at LH.	57
Table 6.5:	The average intraleaf transmission percentage the intraleaf leakage test procedures for both CMJAH and LH for all imaging devices.	59
Table 6.6:	The average intraleaf transmission percentage for the combined test procedures intraleaf leakage results at both CMJAH and LH for all imaging devices.	59

ABBREVIATIONS

A

AAPM American Association of Physicists in Medicine

Am-Si Amorphous Silicon

C

cm centimetre

cGy centigray

CAPCA Canadian Association of Provincial Cancer Agencies

CMJAH Charlotte Maxeke Johannesburg Academic Hospital

CPQR Canadian Partnership for Quality Radiotherapy

CT Computer Tomography

D

3-D CRT 3-Dimensional Conformal Radiation Therapy

E

EPID Electronic Portal Imaging Device

G

Gy Gray

I

IMRT Intensity Modulated Radiation Therapy

L

LANTIS Local Area Network Treatment Information System™

LH Livingstone Hospital

Linac Linear Accelerator

M

MLC Multileaf Collimator

MU Monitor Units

MV Megavoltage

Q

QC Quality Control

QA Quality Assurance

S

SSD Source to Surface Distance

T

TG Task Group

TLD Thermo Luminescent Dosimeters

TV Target Volume

U

UIP Universal IMRT Phantom

V

VMAT Volumetric-Modulated Arc Therapy

1. INTRODUCTION AND AIMS:

Linear accelerators (Linacs) produce high energy photon and electron beams via the acceleration of electrons by high-frequency electromagnetic waves within a waveguide powered by a magnetron or klystron¹. Conventional Linacs are fitted with two sets of solid metal collimator jaws for secondary collimation in high energy photon radiotherapy. These standard jaws are capable of producing divergent rectangular field shapes of up to a 40 cm by 40 cm defined at the treatment distance¹. Most tissue within the rectangular field shape produced by the collimator jaws will be treated including any radiation sensitive normal tissues in the field. To spare normal tissues during a radiation therapy treatment on a conventional Linac, lead or lead alloy shielding blocks are used. Lead-alloy facilitates patient-specific fabrication of these blocks. Limitations of blocks are their time-consuming production, toxic fume emission during the melting and moulding process, and the fact that they can be cumbersome².

Multileaf collimator (MLC) systems were introduced into Linacs in the 1980's³. Currently most manufacturers of teletherapy machines offer the MLC as an option on their units. The main reasons for the introduction of the MLC system were to facilitate computer-control and verification of complex treatment field shapes and to obtain an increase in the speed of both set up and treatment of patients^{1,2}. With MLCs in place, beam-shaping blocks for the most part are no longer needed. There are several MLC collimator jaw configurations available but in general MLC systems consist of 20 – 80 pairs of movable leaves which project a width of 1 cm or less at the treatment beam isocentre². MLC leaf position and speed must be automatically uploaded, verified and controlled by a computer system¹.

MLCs and shielding blocks are used both for shielding sensitive organs in treatment fields and for conforming fields to a target volume. 3-Dimensional Conformal Radiation Therapy (3-D CRT) is a treatment technique in which 3-D anatomical information from a Computed Tomography (CT) scanner is used to produce a highly conformal dose distribution to the target volume (TV). The high conformity of the dose distribution to the target volume must fulfil the dual requirement of sufficient dose to the tumour and achieve as low as possible dose to any normal or radiation sensitive tissue¹.

When using a MLC system, there are inherent challenges:

1. The MLC leaves have a finite width at isocentre. Therefore, when conforming to an irregular shape, there is a limited radius of curvature which is not a concern with cerrobend blocks.
2. Owing to their finite width, the MLC leaves can only be positioned around a non-rectangular tumour with each leaf aligned at its midpoint to the target edge, completely within the target or completely withdrawn from the target.
3. The MLC leaves cannot extend into the target area, thus the MLC are unable to easily replicate an island block¹. The only way to replicate island blocks is to produce multiple matched fields with the leaves from alternating leaf banks closing the field up to and including the island block area during each sub-treatment of the field. Matching across target volumes is usually avoided so treatment with an MLC is a sub-optimal approach in this instance.
4. As the MLC adds or replaces a jaw, all collimator mounted beam-modifying devices (e.g. wedge, tissue compensators, etc.) are fixed in their orientation relative to the MLC.
5. Cerrobend blocks are cut and moulded to be continuous with the Linac beam divergence. Thus, they diverge correctly with the light and radiation fields of the Linac. This is known as dual-focus however most MLC systems are not designed with dual-focus ability.
6. There may be a loss of penumbra from the decreased source-collimator distance when a MLC is added.
7. Additional Quality Control (QC) for the Linac and Quality Assurance (QA) of the MLC itself are required, due to the difference in complexity compared to standard jaws.

Even with these limitations the MLC leaves have an additional ability to be moved to different orientations while the Linac unit is irradiating and/or moving and this leads to an extension of 3-D CRT. This extended use of the MLC capacity allows the delivery of Intensity Modulated Radiation Therapy (IMRT) and a further extension of the IMRT technique such as Volumetric Modulated Arc Therapy (VMAT). IMRT is a treatment technique in which non-uniform radiation beam intensities are delivered from multiple treatment beam positions⁴. Whereas, VMAT is a treatment technique in which the IMRT technique is delivered with the radiation beam continuously on and the Linac gantry rotating for one or more complete arcs⁵.

The implementation of these new techniques with an MLC system and the differences encountered between the solid metal collimator jaw pairs and an MLC system therefore require a re-evaluation of the QA requirements for beam collimation and treatment techniques. An analysis of relevant and recommended QA programs is necessary to determine the optimum requirements and procedures.

The aim of this study is therefore to perform, compare, quantify and evaluate the accuracy of QA efforts for conventional Multileaf Collimators (MLC) installed on medical Linacs.

2. LITERATURE REVIEW

The 2001 American Association of Physicists in Medicine (AAPM) ‘Report no. 72: Basic Application of Multileaf Collimators’², discussed the different MLC configurations available and suggested a preliminary QA program. The 2005 Canadian Association of Provincial Cancer Agencies (CAPCA) ‘Medical Linear Accelerator’⁶ and the 1994 AAPM ‘Comprehensive QA for radiation oncology: Report of the AAPM Radiation Therapy Committee Task Group 40’⁷, both include QA documentation for a Linac. Neither of these documents covered the QA requirements of MLC-equipped Linacs despite widespread use by 2005.

Both associations subsequently released QA documentation to specifically focus on the issue of QA for the MLC. The 2006 CAPCA document ‘Multileaf Collimators’⁸ presents QA for the MLC but does not deal with QA requirements for MLC systems utilized for the treatment of IMRT. In 2009, the AAPM released the ‘Task Group 142 Report: QA of medical accelerators’⁹ document (TG142), which updated the section in the Task Group 40 report⁷ on Linacs, including new technologies such as MLC, asymmetric jaws, dynamic wedge, virtual wedge and electronic portal imaging devices (EPID).

TG142 divides MLC-equipped Linacs into three types; these are non-IMRT, IMRT and those capable of MLC or micro MLC-based Stereotactic radiosurgery/Stereotactic body radiation therapy, with each type requiring different procedures and tolerances on these procedures⁹. The Canadian Partnership for Quality Radiotherapy (CPQR) replaced CAPCA to generate, maintain and inform the QC and QA systems. In 2013, CPQR released ‘Technical Quality Control Guidelines for Canadian Radiation Treatment Centres: Medical Linear Accelerators and Multileaf Collimators’¹⁰ which summarised and combined the 2005 and 2006 CAPCA documents^{6,8}. The TG142 and CPQR documents includes Linac and MLC QC and specifies that it is for non-patient specific IMRT QA.

In 2003, the AAPM released ‘Guidance Document on Delivery, Treatment Planning, and Clinical Implementation of IMRT: Report of the IMRT subcommittee of the AAPM radiation therapy committee’⁴, which was intended to cover the complete process for IMRT from the commissioning of the systems required through to the treatment of patients. This document

suggests QC procedures for MLCs and was used by Charlotte Maxeke Johannesburg Academic Hospital (CMJAH) in the commissioning and implementation of IMRT on their MLC equipped Linac in the Radiation Oncology department. The MLC equipped Linac in the Radiation Oncology department at Livingstone Hospital (LH) does not have IMRT capabilities thus this document was not used in the commissioning of the unit.

The starting point for the methodology and the origin of the test procedures required to produce a comprehensive QA for the MLCs in this study was obtained from this document. The initial procedures for leaf matching, leaf position accuracy and leaf abutment were developed from this document. The document, however, fails to address all the test procedures required for the program to be comprehensive, e.g. intraleaf leakage.

Other investigators developed their own methodologies and test procedures to evaluate the requirements set out by the AAPM and CAPCA^{3, 11-27}. These were based on the type of MLC the authors had at their institutions with only LaSosso¹¹ and Huq, *et al.*²⁴ generalizing with respect to MLC type. Some of these were published prior to the release of the latest AAPM and CAPCA documentation as the awareness for a change in QC procedures grew.

Publications list leaf position accuracy as the major quality assurance aspect of a MLC. Intraleaf transmission is also covered by most authors however; others focused their work only on leaf position accuracy^{13, 17, 19, 20, 27}. Transmission through abutting leaves was only examined by Bayouth¹⁵ and Low, *et al.*²⁵, as these were the only authors using systems with abutting leaves. Only Bayouth¹⁵ examined a Siemens Linac however, the author only discusses leaf abutment but does not suggest how to determine or measure it.

LoSasso¹¹ suggested a QA program for IMRT and presented a thorough examination of the topic. The author suggested how procedures can be executed but did not specify detail. The author defines leaf matching as leaf alignment and suggests that the leaf position accuracy be evaluated separately from leaf alignment.

Half of the publications discussed above as well as the 2003 AAPM⁴ report cover two aspects of the MLC leaf system under the title of leaf position accuracy^{3, 12-14, 17, 18, 20, 23}. These two aspects are the MLC leaf matching and the individual leaf position accuracy. The MLC leaf matching affects the deviation of the distance between the edge of the radiation field defined

by each leaf and the desired field size¹¹. On the other hand, the leaf position accuracy is the accuracy of the individual leaf positions with respect to a reference leaf. The reference leaf is the leaf which is on the isocentric central axis of the collimator system. Some the authors^{15, 19, 22, 25 - 27} only focus on the individual leaf position accuracy of their MLC systems whereas others^{16, 21, 24} only focus on the leaf matching.

The authors use various procedures for the determination of the leaf position accuracy. Lui³ and Baker¹⁷ used a manufacturer-developed system (Elekta) for evaluation of leaf matching and leaf position accuracy called major and minor off-set tests. A strip test technique where the strip test consist of either 2 cm wide fields with 1 mm gap was used by some^{12, 13, 20, 26} whereas 1 cm wide fields with a 1 cm gap was used by others^{15, 19}. Jordan *et al.*¹⁶ and Hounsell *et al.*²³ used fields where alternative methods of producing field sizes of 4 cm x 30 cm are compared. Graves²² used a reference jaw set at 19 cm from the central axis and moved the opposite leaves to different positions with respect to the fixed position jaw. Galvin *et al.*²¹ and Huq *et al.*²⁴ used a 10 cm x 10 cm field size off set in 5 cm steps from the central axis. Parent²⁷ used the same technique but restricted the field size to that of the EPID. Pasquino *et al.*¹⁸ and Low *et al.*²⁵ used six 5 cm x 40 cm abutted fields.

Intraleaf leakage which is also known as the tongue and groove effect is often not discussed at all^{16, 17, 19, 20, 22, 25, 27}. Others^{3, 12, 14, 15} discuss intraleaf leakage but neither gives results nor suggests how to measure it. Jordan *et al.*¹⁶ and Hounsell *et al.*²³ measured intraleaf leakage by completely closing each leaf bank separately in turn. Pasquino *et al.*¹⁸ measured intraleaf leakage by extending alternative adjacent pairs of leaves from each leaf bank and then repeating the pattern for the leaves not extended originally. Others^{21, 24, 26} measured intraleaf leakage by exposing a 10 cm x 10 cm field completely closed by the MLC only and then comparing with an open field. LoSasso *et al.*²⁶ also used an ionization chamber at central axis and in an offset position with open and closed 10 cm x 10 cm fields. Various other field sizes were also investigated. As seen with leaf position accuracy there is no common procedure used for intraleaf leakage.

Most authors used planar imaging for data capture and analysis. There is therefore a need to produce effective, explicit and versatile procedures executable on all MLC types as well as detail the design, methodology and execution of the test procedures. This is pressurized by the continual emergence of new techniques incorporating increasingly complex MLCs that

assumes consistent performance.

QC procedures require not only that the MLC system be evaluated but that data captured and the analysis and archive tools are consistent, reproducible and reliable for maintaining records. Several different detector systems have also been developed for performing QC procedures on MLCs for IMRT delivery. These can be divided into point dose or 1-D, 2-D and 3-D systems with each having inherent advantages and disadvantages.

Point dosimeters are ionization chambers and solid state detectors. Ionization chambers are regularly used for absolute and relative dose measurements in radiotherapy. Solid state detectors are either diodes or thermo luminescent dosimeters (TLDs). The disadvantage of common ionization chambers is the size of the sensitive measurement volume of the ionization chamber relative to the small size of the treatment fields, especially in IMRT and stereotactic work^{28, 29}. This issue is also prevalent in the measurement of steep dose gradients and dose profiles of small fields (IMRT) as discussed by Bouchard *et al.*^{30, 31}. Diodes are used for relative dose measurements for IMRT and produce immediate measurement results. The disadvantages of diodes are directional and dose rate dependence as well as long term radiation damage requiring recalibration and eventual replacement^{28, 29}. TLDs are used for relative dose measurements and demonstrate a high sensitivity within a small volume^{28, 29}. The disadvantages of TLDs are the need for careful calibration, detector specific sensitivity coefficients, a decrease in response over time and a delay in obtaining dose results^{28, 29}. Point dosimeters can only be used to verify local absolute dose delivered within the area of the procedure.

2-D dosimetry systems include radiographic film (wet film), radiochromic film, electronic portal imaging devices (EPIDs), diode arrays and ionization chamber arrays. The radiographic film, radiochromic and EPIDs are all used for relative dose distribution measurements. The advantages of radiographic film are high spatial resolution, accurate and reproducible response, long term data storage and traceability. The disadvantage of radiographic film is that it requires a stable wet chemical processor to develop the film and not all departments have access to these units. The advantages of radiochromic film are as for radiographic film however, radiochromic film does not require chemical processing. The disadvantage of radiochromic film is the low sensitivity with the current Gafchromic EBT series having sensitivity similar to the Kodak EDR-2 radiographic film as discussed in Low

*etal*²⁸ and Marinello²⁹. The advantages of the EPID are time saving compared to film and a better spatial resolution than array detectors. The disadvantages of the EPID are limitations in the field size, the need for multiple signal corrections to obtain dose results in the detector and the requirement for commercial software packages for automated result analysis²⁸. Diode and ion chamber arrays can be used for routine QC of the MLC. The advantages of the arrays are the number of dose measurement points achievable from a single exposure and the immediate availability of the results. The disadvantages of the arrays are a low spatial resolution, uniformity and the need for regular calibration (monthly for some devices)^{28, 29}.

3-D systems are polymer, Fricke and radiographic gels and plastics as well as a combination of detectors in anthropomorphic phantoms. The advantages of all the 3-D systems are the production of a 3-D dose distribution, correct anatomical shaping for IMRT plan QA and high spatial resolution. The disadvantages of the gel and plastics systems are the high cost, complexity and time duration required to obtain results^{28, 29}. The disadvantages of the anthropomorphic phantoms used in conjunction with detectors are the requirement for appropriate analysis software, registration of the measured and calculated dose distributions and correct alignment within the software to maintain correct anatomical dosimetric information^{28, 29}.

In summary, there is a need not only for a comprehensive QA program for the MLC system but also for an accurate, efficient and effective method of data capture and an independent analysis methodology that best fits the resources available. Due to the complexity and advanced functionality of the MLC over conventional collimation systems, the QA requirement for MLC-based Linacs needs to be expanded accordingly.

3. MATERIALS

The procedures, methodology and dosimetry systems relevant to an informative QA program for an MLC on a medical Linac were selected based on the resources available at each site.

3.1 Multileaf Collimators

Two MLC collimator configurations were examined and studied in this work.

In the first configuration the conventional upper solid secondary collimator jaws are replaced with two opposing banks of 40 leaves per bank and a set of solid back-up jaws (diaphragms) positioned immediately below the leaves. Each back-up jaw automatically positions at the outer most leaf position. This configuration is currently used by Elekta (Pty) Ltd for their Linac units and is available at Livingstone Hospital (LH) in Port Elizabeth. Each MLC leaf can travel beyond the central axis by 12.5 cm and therefore each leaf can move through a total distance of 32.5 cm to produce a maximum open field size of 40 cm x 40 cm at the isocentric plane. The single-focussed MLC leaf pairs have a minimum separation of 5 mm and are unable to abut owing to their rounded leaf edges². The opposing leaf pairs project a width of 1 cm each at isocentre and IEC 61217 naming convention is applied.

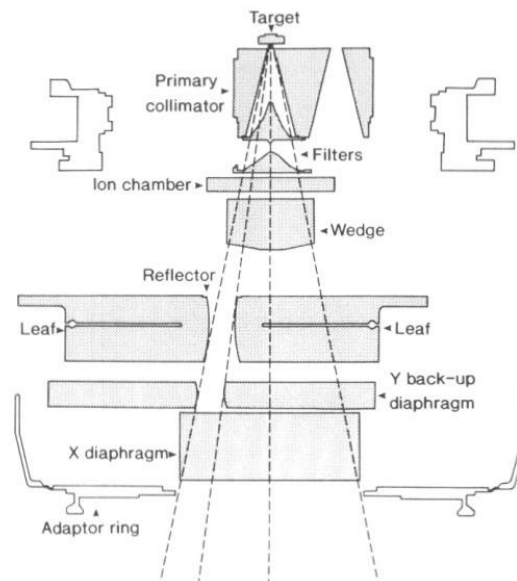


Figure 3.1: Diagram of Elekta Linac jaw and leaf orientation in the Linac collimator head as used at LH. (Image found in Jordan *et al.*¹⁶)

In the second configuration, the MLC replaces the conventional lower solid secondary collimator jaws with two opposing banks of 41 leaves each. This configuration is currently used by Siemens (Pty) Ltd for their Linac units and is available at CMJAH. Each MLC leaf can travel beyond the central axis by 10 cm and therefore each MLC leaf can move a total distance of 30 cm to produce a maximum open field size of 40 cm x 40 cm at the isocentric plane. The leaves in this configuration have leaf ends and sides which are continuous with the divergence of the radiation beam. This design configuration is known as double focused. The double focused leaf edges are straight and the leaves can thus abut. The leaves could also be independently and manually controlled via the hand controller of Linac control system². The opposing leaf pairs project a width of 1 cm each at isocentre and the IEC 61217 naming convention is applied.

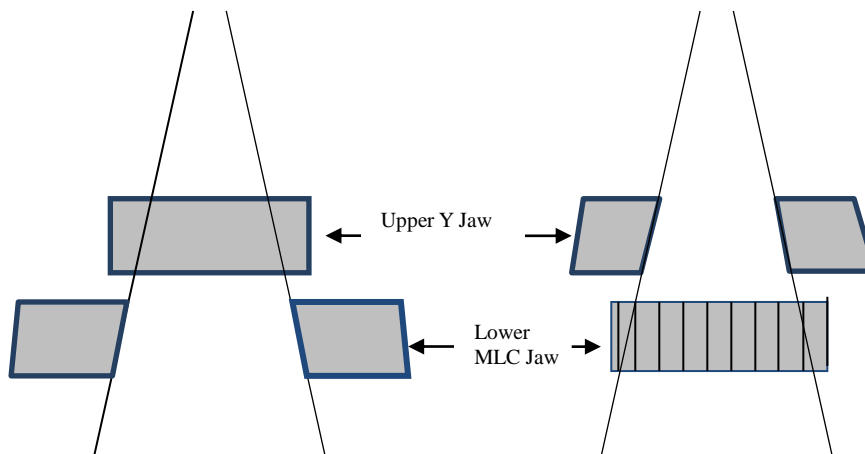


Figure 3.2: Diagram of Siemens Linac jaw and leaf orientation in the Linac collimator head as used at CMJAH.

These configuration aspects affected the design and implementation of the leaf position accuracy and abutment test procedures as they were required to be carried out on both platforms for direct comparison.

3.2 Megavoltage 2 Dimensional Detectors

Three imaging devices were used:

The first of these was wet film or radiographic film, which required chemical developing in a wet processor. Two batches of the Kodak X-Omat VTM series of film of size 25.4 x 30.5 cm²

were used. A Konica Minolta SRX-101A wet processor was used at CMJAH and a KODAK Medical X-ray Processor 102 at LH.

The second was radiochromic film; this means that the film colours directly when exposed to radiation and does not require chemical development. Two sizes and batches of Gafchromic EBT2 series of films were used: 35.6 x 43.2 cm² and 20.3 x 25.4 cm².

The third was the Electronic Portal Imaging Device (EPID), which is a Linac gantry mounted real time imaging device. The EPID in LH is constructed from amorphous silicon (aSI) flat-panel detectors and had a fixed SID of 160 cm. The EPID array size was 41 x 41 cm² and therefore could image a maximum field size of 26 x 26 cm² at isocentre¹⁷.

3.3 Ionization Chambers

The ionization chambers which were used in CMJAH were a PTW LA48 linear array system and calibrated cylindrical ionization chambers of different volumes (PTW 31010 0.125 cm³ Semiflex chamber and a PTW 30010 0.6 cm³ Farmer chamber). All were calibrated in terms of IEC 60731. The linear array had an active measuring length of 37 cm and consisted of 47 fluid filled 8 mm³ ionization chambers. These ionization chambers were each 4 mm x 4 mm x 0.5 mm spaced 8 mm apart on the central plane of the array. The linear array was used with the PTW MP-3 water tank system and the MEPHYSTO mc² acquisition software. The array was moveable laterally such that a 1 – 8 mm measurement resolution could be achieved.

The detectors used in LH were a PTW 31010 0.125 cm³ Semiflex chamber and a PTW 30013 0.6 cm³ Farmer chamber. Both were calibrated in terms of IEC 60731. The cylindrical ionization chambers were used to obtain the absolute dose values required for the calibration of the films.

3.4 Phantoms

The acrylic PTW Universal IMRT phantom (UIP) (Figure 3.3) was used for the film measurements at CMJAH. The phantom consists of 2 interlocking sections, the top section was a 30 x 30 x 5 cm³ plate scribed with centre marking to aid setup and 5 film prickers for localization and orientation. The second section has a 30 x 30 x 2 cm³ plate which was

scribed with centre marking and 5 holes with plugs at 1 cm depth. The holes are designed to accommodate a 0.125 cm^3 cylindrical chamber. The film was placed between the 2 acrylic plates.

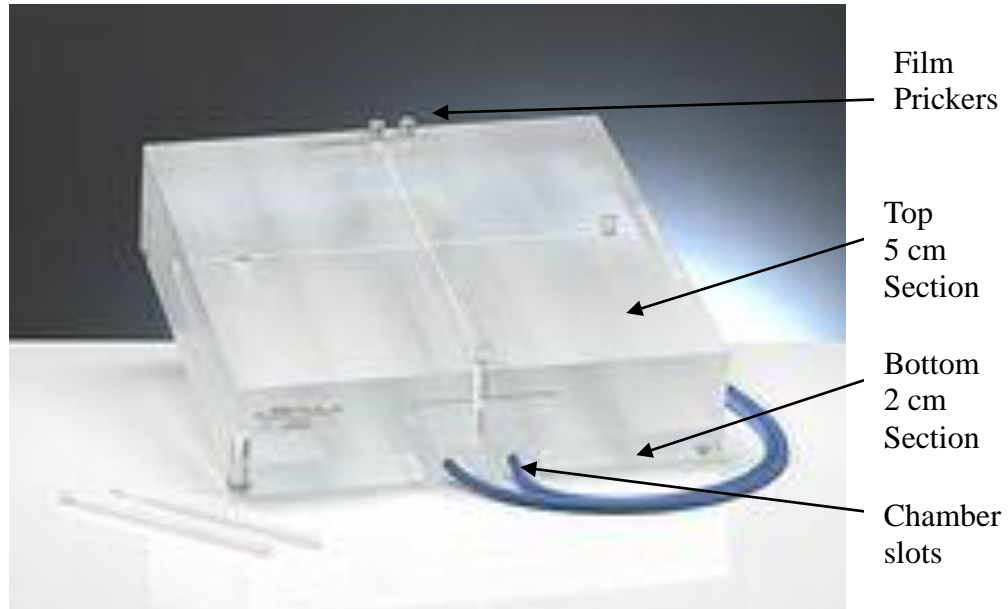


Figure 3.3: Universal IMRT phantom structure indicating the film prickers, the chamber slots and the two sections of the phantom.

At LH a $30 \times 30 \times 7 \text{ cm}^3$ phantom consisting of 1 cm thick pieces of polystyrene was used for the film set. The same materials for both phantoms were not available at CMJAH (UIP acrylic) and LH (polystyrene sheets). The films were thus placed at 5 cm depth at LH to reproduce as closely as possible the position used at CMJAH in the UIP. A separate $30 \times 30 \times 1 \text{ cm}^3$ plate with a hole for a 0.125 cm^3 cylindrical chamber was used in the phantom when point dose measurements were required.

No phantom was used for the images obtained with the EPID systems.

3.5 Film Scanners and Dosimetric Software

An Epson 10000 film scanner was used to capture the dosimetric information from the wet radiographic and radiochromic films into a digital format in CMJAH and a Microtek Scanmaker 9800XL film scanner was used in LH. The acquisition settings of the Epson scanner for the wet film were 16-bit grey scale and 400 dpi, and for the radiochromic films

the settings were 48-bit colour and 400 dpi. All colour corrections were switched off. The same settings were used on the Microtek scanner.

The Film analysis software PTW VerisoftTM was used for analysis and comparison of the dosimetric information obtained from the wet film, radiochromic film, EPID and the ionization chambers.

4. METHODOLOGY

4.1 Experimental Test Procedures Introduction

AAPM TG142 lists recommended QC test procedures which need to be carried out for an MLC used in both IMRT or non-IMRT modes⁹. The 2013 CPQR ‘Medical Linear Accelerators and Multileaf Collimators’ lists all the test procedures required for a Linac with an MLC¹⁰. As discussed in chapter 2 the major annual QC test procedures are leaf position accuracy, intraleaf leakage and transmission through abutting leaves. For this thesis leaf position accuracy was separated into leaf matching and leaf position accuracy. These 4 test procedures were therefore conducted in this work. In addition, a leaf sequence that combines and examines all the test procedures was also designed and investigated.

4.2 Quality Control Test Procedures Design

All test procedures were produced, set up and executed from a record and verify data management intranet system at both CMJAH (using the LANTIS™ system) and LH (using the MOSAIQ™ system) to maintain reproducibility, increase procedure speed and provide a record of the test procedure. All the test procedures at CMJAH were conducted using the 6 MV photon energy beam and all the test procedures at LH were conducted using the 8 MV photon energy beam. These energies were selected since they are the most commonly used at each site.

4.2.1 Leaf matching test procedure

Leaf matching affects the deviation of the distance between the edge of the radiation field defined by each leaf and the desired field size¹² as discussed in chapter 2. Inaccurate leaf matching alters the dose homogeneity between adjacent fields. The examination of this effect was tested by setting up a sequence consisting of six 5 cm x 40 cm field strips each irradiated with the same MU setting shown in figure 4.1. Both MLC designs were capable of delivering this test procedure and in LH the test procedure was conducted with the back-up jaw in the field and the back-up jaw out the field. The MLC leaves would define the field edge when the back-up jaws are out of the field. Thus demonstrating the effect of the back-up jaw on the

test procedure. Perfect MLC performance should result in a uniform field of 30 x 40 cm² at isocentre. The recommended tolerance is 1 mm and action level is 2 mm¹⁰.

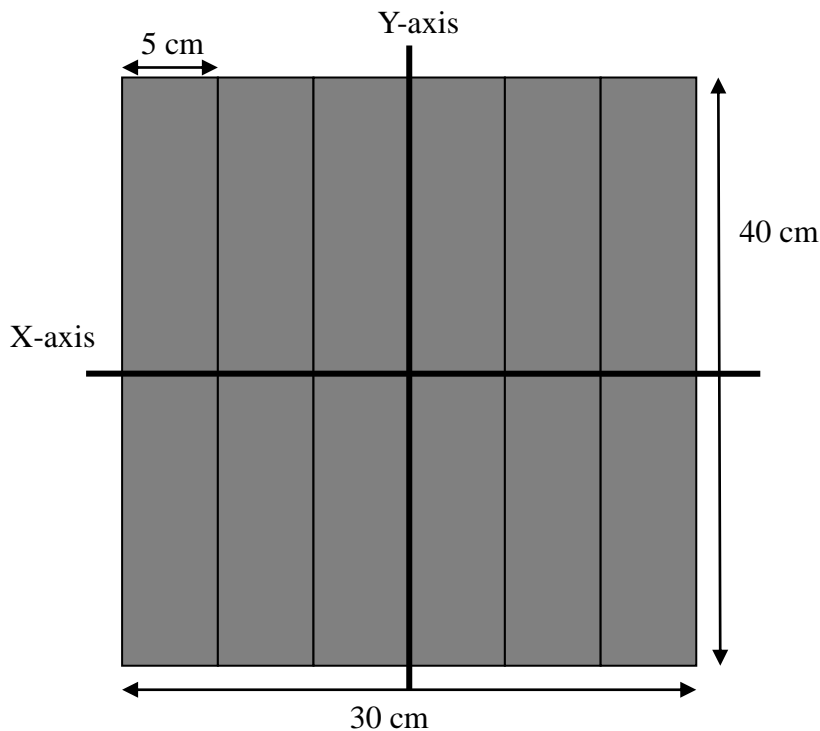


Figure 4.1: Diagram of leaf matching test procedure.

4.2.2 Leaf position accuracy test procedure

The edge of each MLC leaf may have to move to multiple positions during a treatment and the accuracy of this movement to the set position will define the accuracy with which a specified field shape can be reproduced. The positional accuracy of each leaf should be maintained over the full travel of the leaf as well as from both a positive and negative directional approach.

The leaf position accuracy test procedure at CMJAH consists of fields of 2 mm x 40 cm strips at 2 cm intervals across the MLC travel, which produces a composite field of 20.2 x 40 cm². The leaf position accuracy test procedure at LH consists of 5 mm x 40 cm thick strips at 2 cm intervals across the maximum MLC over travel, which produces a composite field of 24 x 40 cm². The 5 mm strip width used at LH arose from the Elekta MLC system having round ended leaves preventing abutment and thus the smallest separation between opposed leaves

allowed is 5 mm.

Since these two test procedures could not be compared directly, the leaf position accuracy test procedure for this study was re-configured to consist of 7 field strips of 2 cm x 40 cm thick. The field segments were spaced at 2 cm intervals for the outer two sets of strips and reduced to 1 cm on either side of the central axis strip as shown in figure 4.2

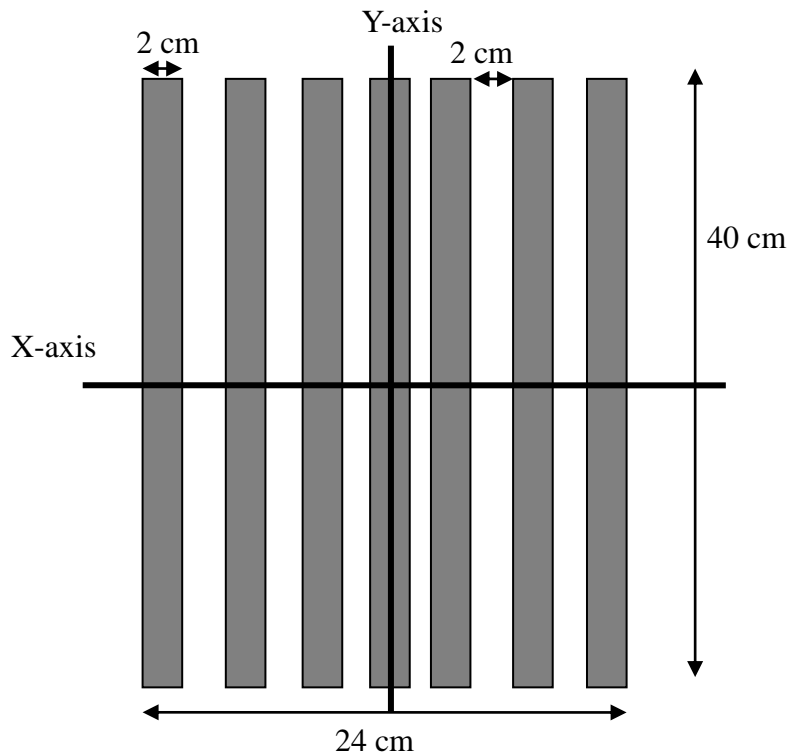


Figure 4.2: Diagram of leaf position accuracy test procedure predicted result for the comparison between CMJAH and LH in this study.

4.2.3 Intraleaf leakage and abuttal test procedures

An MLC that can abut completely should permit the same level of transmission as a closed solid jaw system. The abuttal leakage is of greater importance for IMRT treatment than 3-D CRT as the outputs used are higher. Abuttal leakage of the leaves may also be called interleaf leakage as it is the leakage between corresponding leaves on opposing leaf banks.

MLC leaves are also required to move parallel to each other and a transmission of $< 5\%$ through shielded areas is recommended as per solid collimator jaws¹ and the recommended

tolerance is that they should vary only $\pm 0.5\%$ from baseline⁹. To minimize intraleaf leakage (between leaves in the same bank) the MLC leaves are designed to overlap and this is commonly known as the “tongue and groove” configuration. This is schematically shown in figure 4.3. Transmission increases with higher energies, and is more significant in IMRT when higher outputs are used and a measurable dose is delivered to the shielded parts of each field segment.

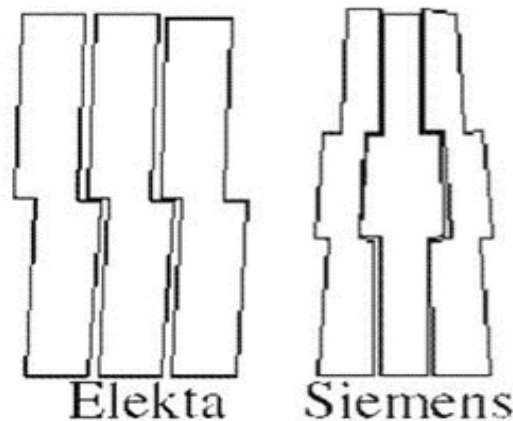


Figure 4.3: Diagram of the Elekta and Siemens MLC systems indicating the tongue and groove leaf configuration (Image found in Huq *et. al*²⁴).

The sequence used to test abuttal and intraleaf leakage consisted of three field segments. In the first segment the leaf banks were closed together at a position of -10 cm from central axis, in the second the leaf banks were closed on the central axis and in the final segment the leaf banks were closed at +10 cm from the central axis. The central leaf (leaf 21 on Siemens at CMJAH and 20 on Elekta at LH) was left open for all segments to deliver a dose to which the intraleaf leakage could be compared. A schematic of the CMJAH procedure is shown in figure 4.4 and LH is shown in figure 4.5. The LH test procedure was different as the system was unable to abut the leaves and a 5 mm gap was necessarily present between opposing leaves. The sequence was however still valid for testing the intraleaf leakage.

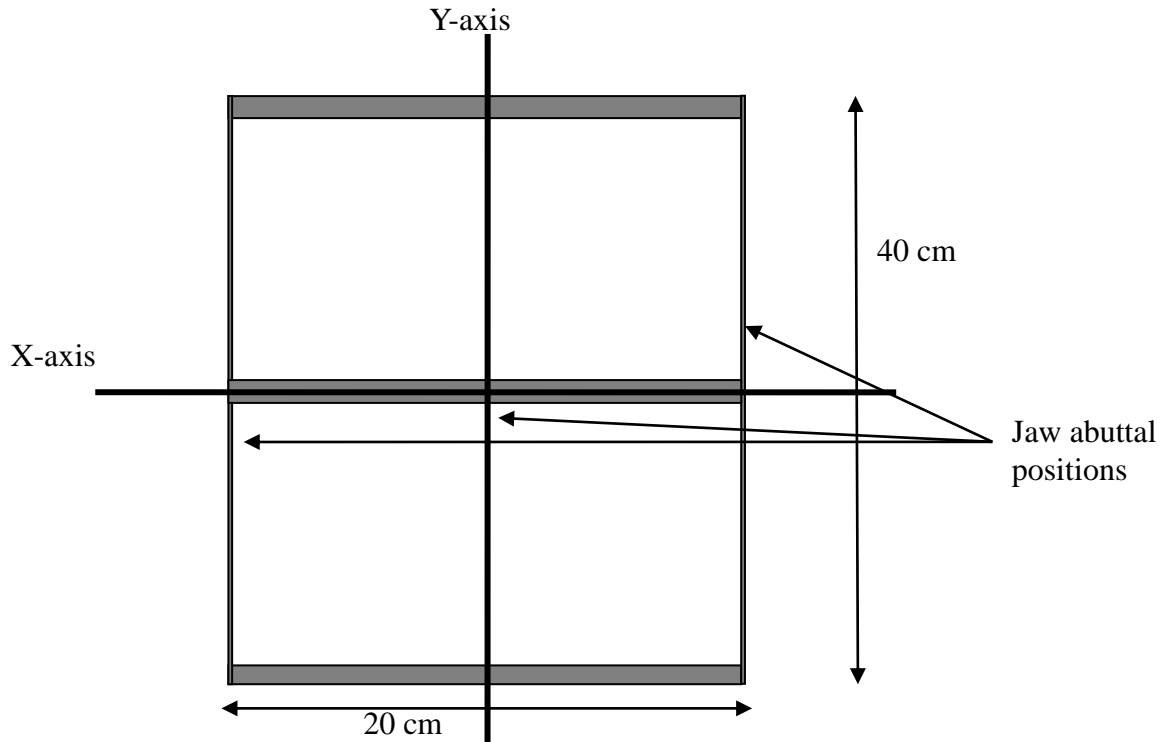


Figure 4.4: Diagram of intraleaf leakage and abuttal test procedures for CMJAH. The thicker grey horizontal area indicates open leaves.

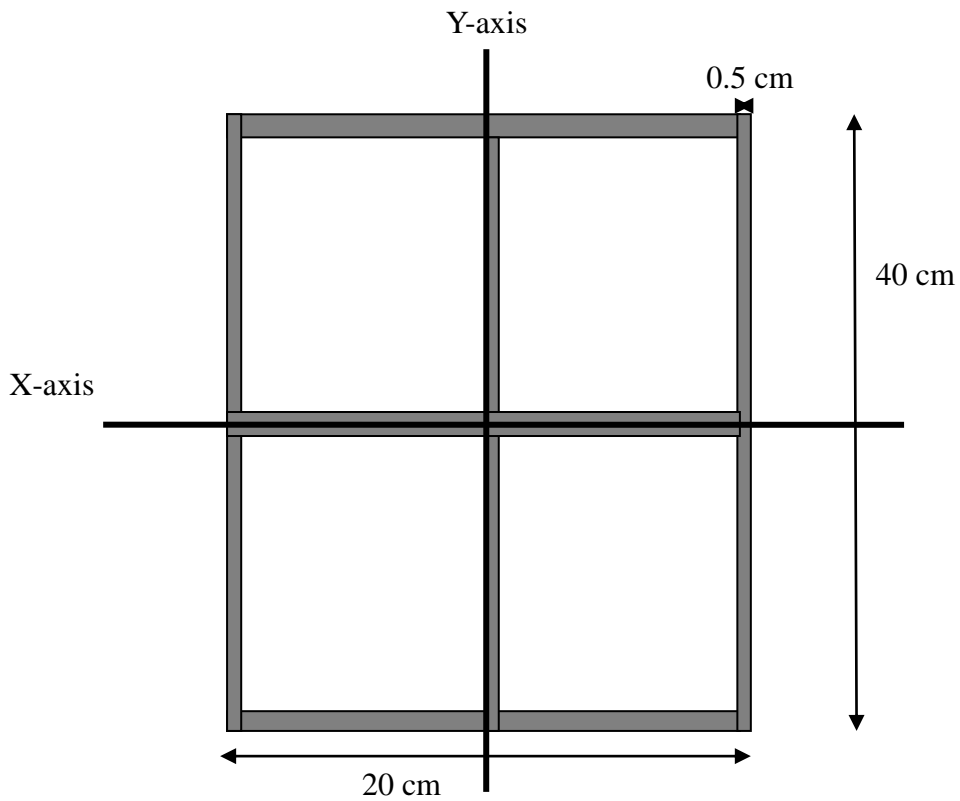


Figure 4.5: Diagram of the intraleaf leakage test procedure for LH. The thicker grey horizontal area indicates open leaves.

4.2.4 Combined test procedure

A single pattern was designed to combine all the test procedures and establish if it is possible to obtain equivalent results. The combined test procedure as shown in figure 4.6 consisted of 7 field segments which included the four individual test procedures. The test produces a composite field size of 25 x 40 cm². The leaf matching capabilities of the MLC was examined by producing four 2.5 cm x 20 cm fields with each field off set from the central axis by either 11.25 cm or 8.85 cm in both the negative and positive travel directions. The leaf position accuracy capabilities of the MLC were examined from three 2 cm x 40 cm fields, at the central axis and 1 cm apart on either side. The intraleaf and abuttal capabilities were examined using the non-irradiated portion of the composite field between the leaf matching and leaf position accuracy segments.

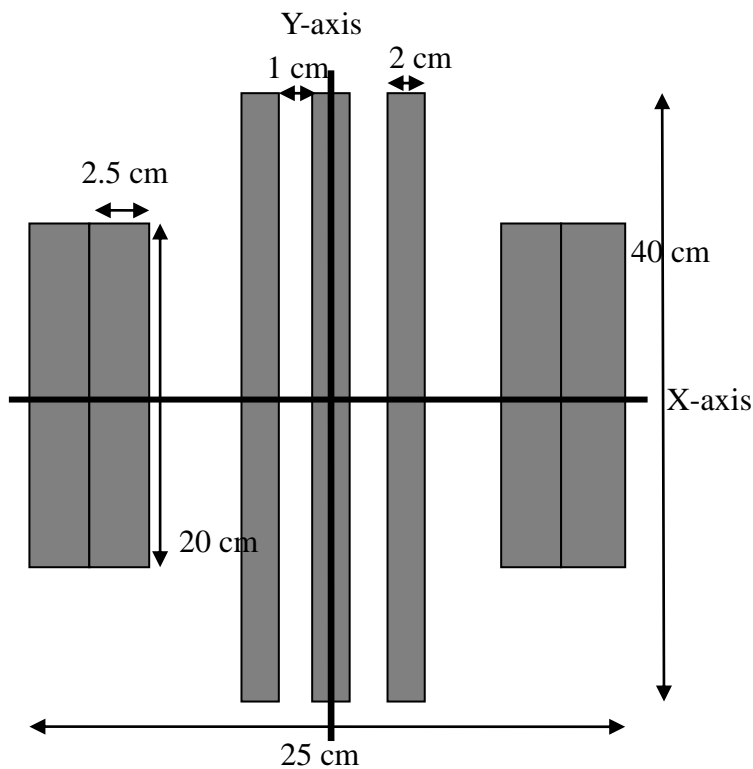


Figure 4.6: Diagram of the combined test procedure consisting of segments for leaf matching, leaf position accuracy, intraleaf leakage and abuttal test procedures.

4.3 Megavoltage 2 Dimensional Detectors and Linear Array Setup and Calibration

The physical differences between the planar detectors and the linear array required different methods related to the physical dimensions of the devices, the dose range and response.

4.3.1 Radiographic film

The maximum field size that needed to be examined was $30 \times 40 \text{ cm}^2$ when conducting the leaf matching test procedure but the Kodak X-Omat VTM that was available had dimensions of $25.4 \times 20 \text{ cm}^2$ thus a single film could not be exposed at isocentre (100 cm from the source). The Universal IMRT (PTW) phantom in CMJAH was therefore setup with the film at isocentre as shown in Figure 4.7 and then the table of the Linac was raised through 32 cm so that the film to source distance was 68 cm as shown in figure 4.8. These set up conditions were used as the field light of the $30 \times 40 \text{ cm}^2$ field size covered the films radiation sensitive area and was as close to the accessory tray of the Linac to still allow for films to be changed without the need to move the complete set up. All test procedure films except the leaf matching test procedure were conducted at isocentre as their field sizes were less than or equal to 25 cm. A similar setup was used at LH. Figure 4.9 and figure 4.10 show the isocentric and the Source to Surface Distance (SSD) of 63 cm set ups at LH respectively. The SSD 63 cm set up maintains the film to source distance of 68 cm as used at CMJAH.



Figure 4.7: The positioning of the UIP for the exposure of films at the isocentre of the CMJAH Linac.



Figure 4.8: The positioning of the UIP for the exposure of films at the SSD 63 cm setup for the CMJAH Linac.



Figure 4.9: The positioning of the Polystyrene phantom for exposure of films at the isocentre of the LH Linac



Figure 4.10: The positioning of the Polystyrene phantom for the exposure of the films at the SSD 63 cm setup for LH Linac.

The dose range, methods of calibration, general recommended handling and processing of the radiographic film used in this study was based on the 2007 American Association of Physicists in Medicine (AAPM) ‘Task Group 69 Radiographic film for megavoltage beam dosimetry’³². The Kodak X-Omat VTM film has a dose response range of 5-100 cGy and a saturation of 200 cGy. Both the Linacs used were calibrated to deliver a dose of 1 cGy per Monitor Units (MU), at isocentre in a 10 x 10 cm² field at the depth of maximum dose. Each irradiated segment of each test procedure was delivered with 30 MU so that the most sensitive dose region of the film was used and the saturation point of the film was not exceeded.

The calibration of the radiographic film was performed at CMJAH using a soft wedge and varying the central axis dose. The resultant dose range used covered the response range of the film. Four films were exposed with a 20 x 20 cm² field size at isocentre at 5 cm depth in the UIP phantom with 10, 20, 50, and 100 MU (total MU delivered to central axis) respectively and a wedge angle of 60⁰. The central axis dose was measured at the same time using the 0.125 cm³ Semiflex cylindrical chamber corrected for temperature and pressure. The combined known central dose and the wedge profile obtained with the LA48 linear array for the same fields were used to determine the dose to various points on the films. This was done

every 1 cm along the central axis in the wedge direction.

The LH Linac has a motorized physical wedge system consisting of a physical wedge of 60^0 angle mounted in the Linac collimator head. The wedge angle is varied by controlling the amount of MU when the wedge is in the field for a completed treatment. Due to the beam hardening effect where lower energy photons are attenuated out of the beam by the wedge¹, the LH films were calibrated using a different method. This method did not use any beam modifying devices such as wedges. Four films were exposed with four open fields each of 7 x 7 cm² field size. The fields were off set to the corners of the film and the rest of the film was shielded. The film was placed at the isocentre at 5 cm depth in a 30 x 30 x 7 cm³ polystyrene phantom and exposed to 0, 1, 2, 5, 10, 15, 20, 30, 50, 70, 100, 150 and 200 MU respectively. The central axis dose was confirmed using the PTW 0.6 cm³ Farmer cylindrical chamber for each exposure.

4.3.2 Radiochromic film

The radiochromic film used was of two different sizes and batches but direct comparison with the radiographic film required that the same setup for exposing both type of films was used.

The Gafchromic EBT2 film has a dose response range of 1 - 4000 cGy. Accordingly, each irradiated segment of each test procedure was delivered with 80 MU so that the exposures were within the most sensitive dose region of the film.

The dose range, methods of calibration, general recommended handling and processing of the radiochromic film was based on the 1998 American Association of Physicists in Medicine (AAPM) 'Report 63: Radiochromic film dosimetry'³³. The calibration of the radiochromic film was carried out using exactly the same setup, positioning and phantoms as used for the radiographic film. The only difference arose in the dose range used as the radiochromic film has a high dose response range. For this study the lower end of the film dose range was used. Thus at CMJAH the films were exposed to 20, 50 and 100 MU with a 60^0 virtual wedge and at LH the films were cut into 10 x 9 cm² pieces and each piece was exposed to 0, 1, 2, 5, 10, 15, 20, 30, 50, 70, 100, 150, 200, 300, 500 and 700 MU respectively.

4.3.3 Electronic Portal Imaging Device (EPID)

The EPID did not require calibration but dose response measurements were conducted to confirm that the dose accuracy and sensitivity of the EPID. The dose response of the EPID was carried out differently from the film dosimetry as the doses used were much lower and no phantom was used for the EPID images. Seven $10 \times 10 \text{ cm}^2$ fields were used for various MU values (1, 2, 4, 8, 10, 15, 20, 50 and 100)¹⁷.

No phantom was used for the EPID data. It was recommended by the manufacturer of the Linac system that single dose exposures for the EPID are less than 4 MU hence all exposures using the EPID were 2 MU per field segment.



Figure 4.11: The position of the EPID for the exposure of EPID images for the LH Linac.

4.3.4 Linear array

The linear array was set up in the PTW MP-3 water tank system at isocentre at a depth of 5.5 cm in water shown in figure 4.12 - 13. This was done to maintain an equivalent depth to the films in phantom. The calibration of the linear array was done with a $20 \times 20 \text{ cm}^2$ 60° virtual

wedge field over 50 MU. The leaf positioning accuracy and leaf matching test procedures were also conducted with the array aligned along the central axis of the MLC leaves, parallel to the direction of travel as well as a 1 cm off set from central axis for the position accuracy. The intraleaf leakage and abuttal test procedures were conducted with the linear array positioned along the Y jaw axis, offset 5 cm from central axis and along leaves 21, 30 and 10. The combined test procedure was carried out and measurements were taken along leaf 21 and 32 as well in the Y direction at an offset of 6.5 cm. All segments of the combined test procedure were exposed for 30 MU and the maximum spatial resolution used for the test procedures was 2 mm.



Figure 4.12: The PTW MP3 water tank, support table and reservoir tank used with the LA 48 at CMJAH.

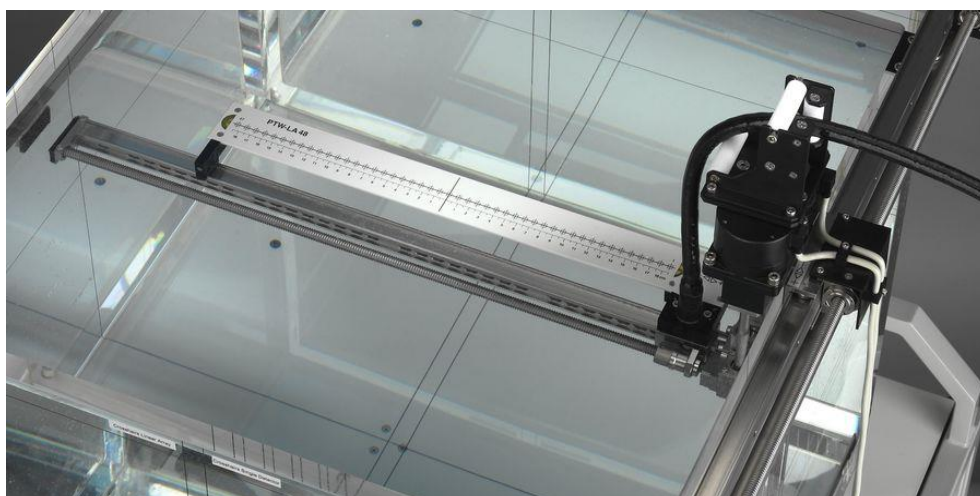


Figure 4.13: The LA 48 set up in PTW MP-3 water tank for the CMJAH Linac.

5. RESULTS

The test procedures were conducted at least twice for each planar detector type at each institution with a minimum time separation of 4 months. The difference in time was to determine if the test procedures could detect changes to the MLC systems over time. It was possible to obtain data over a longer period of time at LH including during an annual major service during which the MLC system was recalibrated.

5.1 Results of the MLC Performance at CMJAH

All results below were obtained at CMJAH on the Siemens Linac using the 6 MV photon beam and the methodology laid out in the previous chapter.

5.1.1 Calibration curves

The radiographic and radiochromic films required that the relationship of dose to optical density ratio be established; this was obtained by the development of a calibration curve. The calibration curves were specific for each detector type, machine and energy used^{32, 33}. Figure 5.1 shows an example of one of the Kodak X-Omat VTM films obtained for the calibration curve. Figure 5.2 shows the calibration curve obtained for the Gafchromic EBT2 film obtained with the methodology discussed previously.

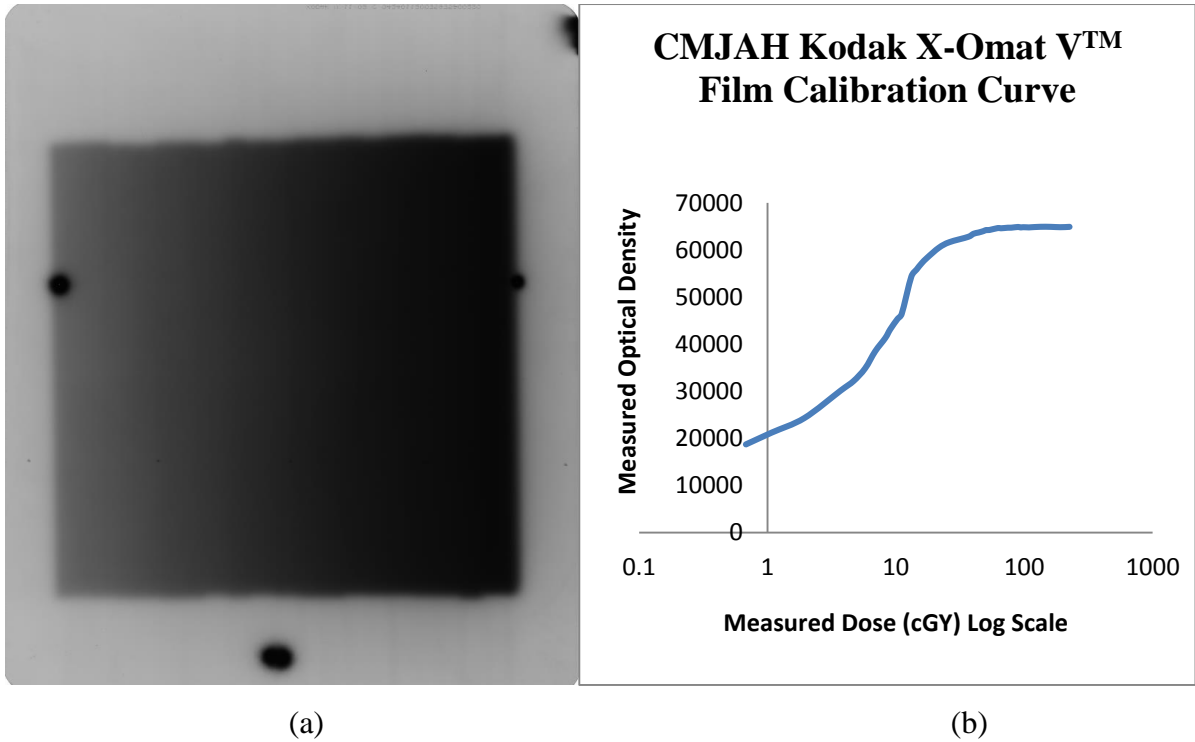


Figure 5.1: Image (a) illustrates the Kodak X-Omat V™ film exposed at CMJAH to a 20 x 20 cm² field size at isocentre in the UIP phantom with 20 MU and a virtual wedge angle of 60° for the purpose of calibration of the the Kodak X-Omat V™ film. Graph (b) is the linear-logarithmic curve obtained when plotting the measured optical density against the known dose for the corresponding MU field.

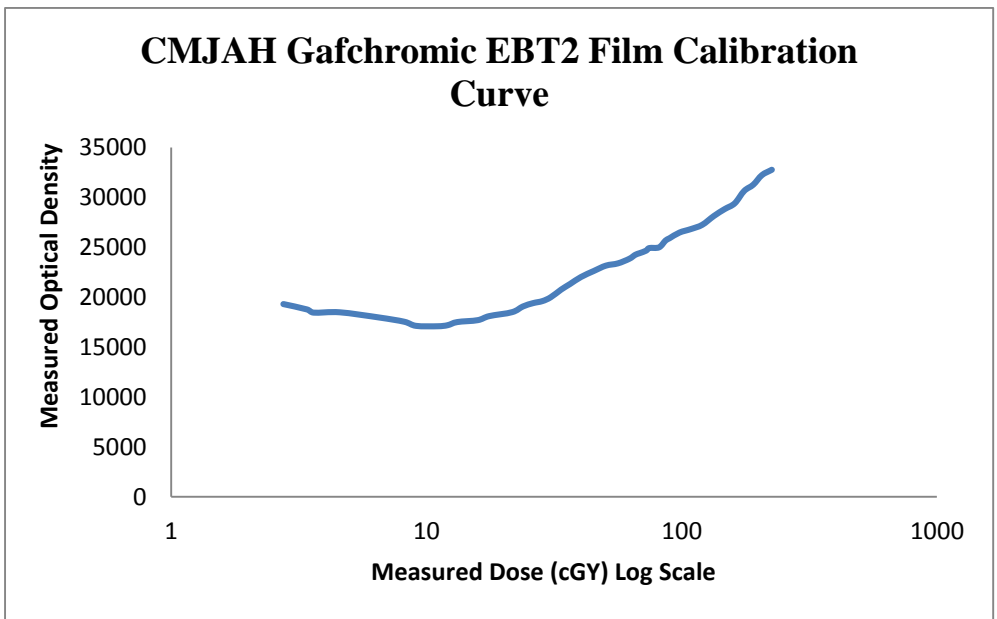


Figure 5.2: The Gafchromic EBT2 calibration curve for CMJAH 6 MV photon beam.

The PTW LA48 linear array was calibrated by the manufacturer. A 60° wedge profile was measured to produce the calibration values for the film and is shown below in figure 5.3.

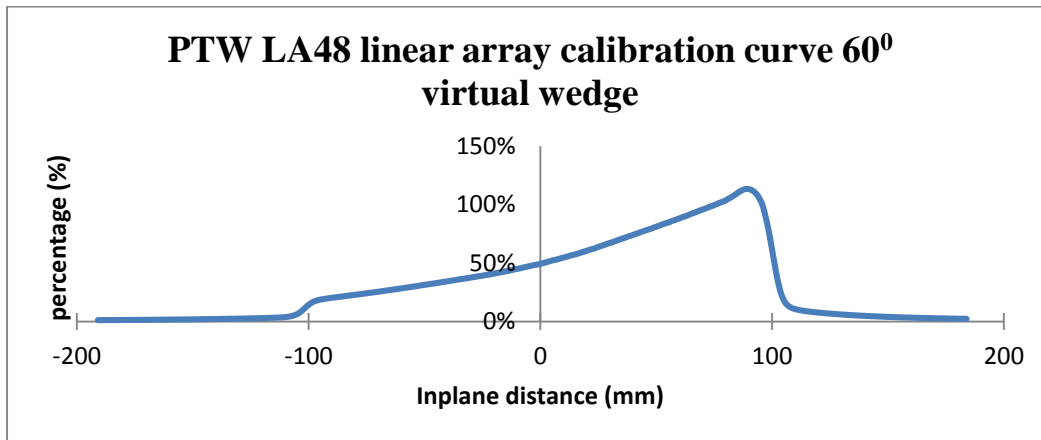


Figure 5.3: The calibration curve from the PTW LA48 Linear array obtained from a 20 x 20 cm² 60° virtual wedge field delivered over 50 MU to the central axis. The curve was measured at a depth of 5.5 cm in water at isocentre.

5.1.2 Quality Assurance test procedure results

An example of the output obtained for each test procedure and the corresponding relevant profile from one of the planar detectors or the linear array are displayed in figures 5.4 – 5.11.

Leaf matching test procedure

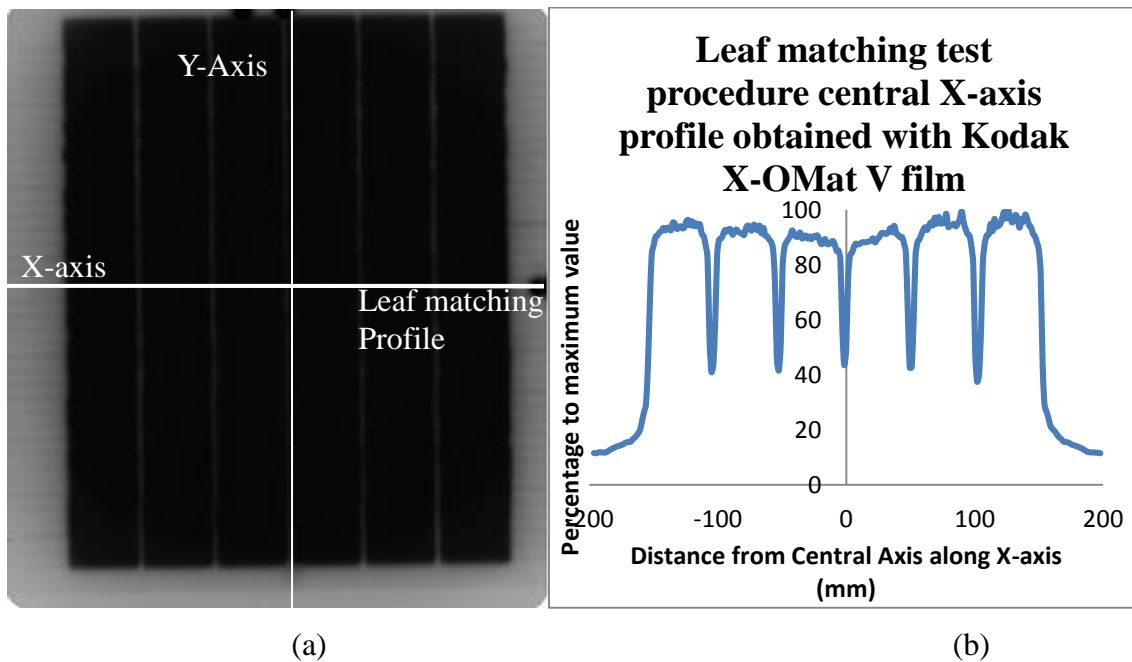


Figure 5.4: Image (a) is the Kodak X-OMat V film of the completed leaf matching test procedure obtained using the UIP phantom at 5cm depth in phantom with the film set up with a SSD of 63 cm for a 6 MV photon beam and 30 MU delivered per field segment. Graph (b) is the profile of the central X-axis as indicated on image (a). The data were obtained using the film calibration data, the MEPHYSTO software and adjusted to represent the field dimensions at isocentre.

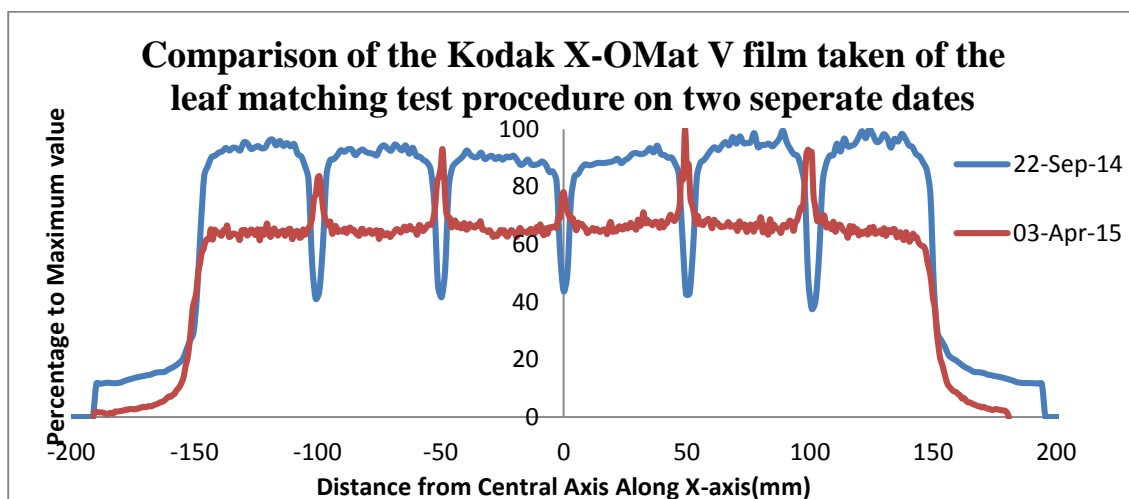


Figure 5.5: A comparison of the profile of the central X-axis produced from the Kodak X-OMat V film on the 22 September 2014 and the 03 April 2015.

As seen in Figure 5.5, the troughs in the older data set indicated that the MLC leaf matching field segments were under travelling the set position thus produced less dose in the overlapping area. The peaks in the newer data indicated that the MLC matching field segments were over travelling the match point thus contributed more dose in the overlapping area. These differences were due to a recalibration of the MLC between the measurements.

Leaf position accuracy test procedure

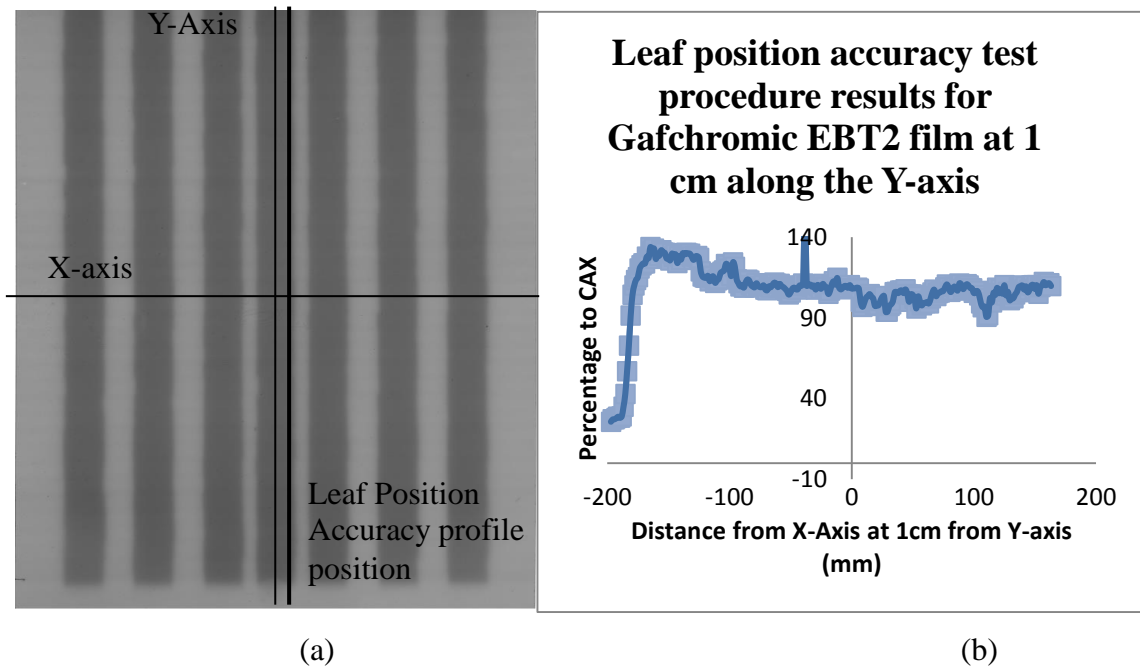


Figure 5.6: Image (a) is the Gafchromic EBT2 film of the completed leaf position accuracy test procedure obtained using the UIP phantom with the film set up with a SSD of 63 cm for 6 MV photon beam and 80 MU per field segment. Graph (b) is the profile of the field defined by the MLC along the central field segment as indicated on image (a). The data were obtained using the film calibration data, the MEPHYSTO software and adjusted to show the field dimensions as defined at isocentre.

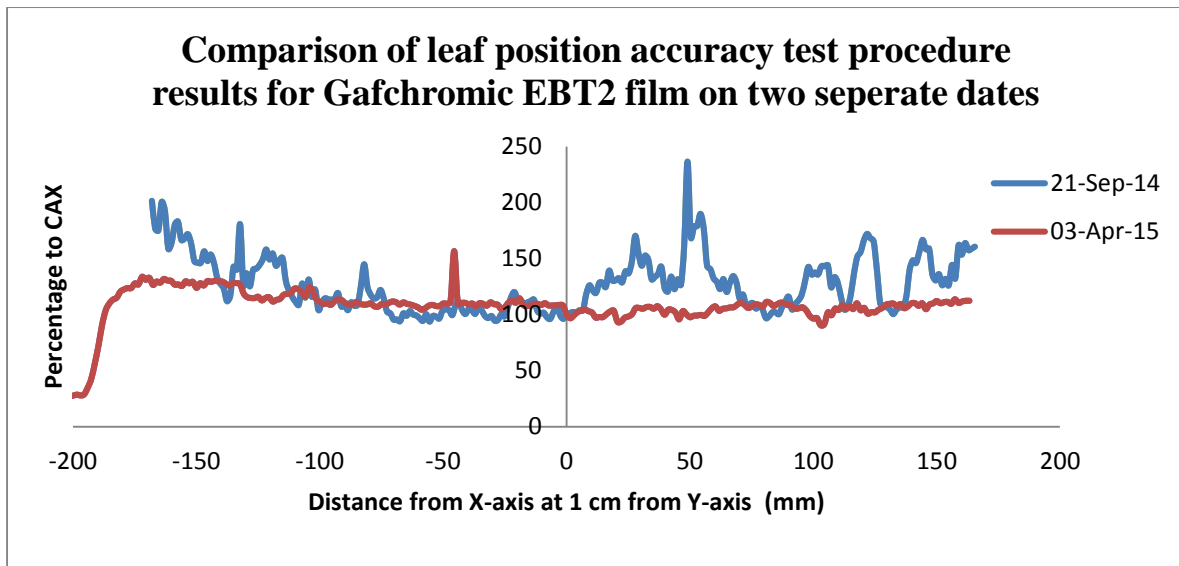


Figure 5.7: A comparison of the profile 1 cm along the Y-axis produced from Gafchromic EBT2 film on the 21 September 2014 and the 03 April 2015.

Intraleaf leakage and abuttal test procedure

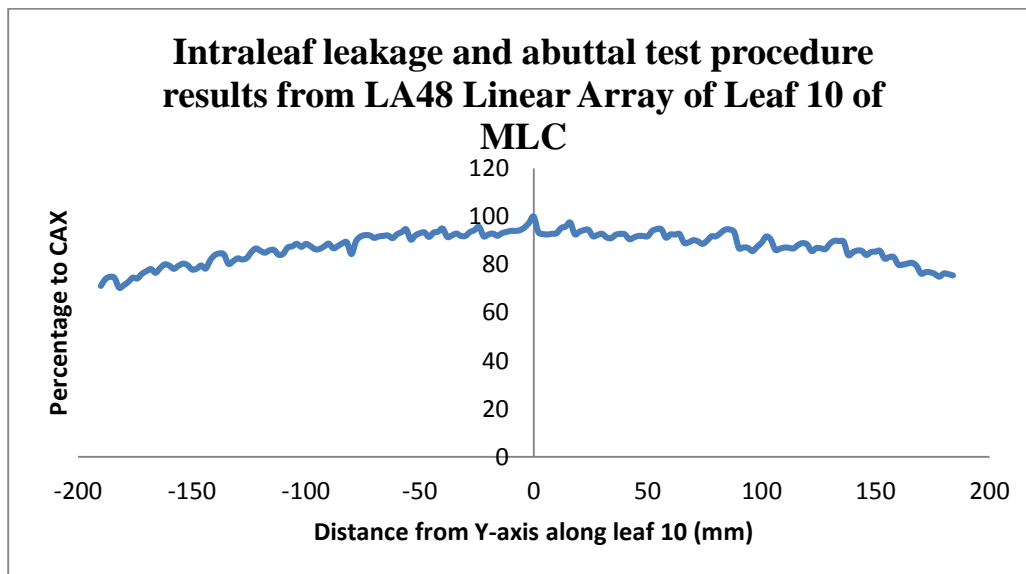


Figure 5.8: The LA 48 Linear array profile of Leaf 10 (5 cm from the central axis) to obtain the intraleaf leakage and perform the abuttal test procedure. A 2 mm step size was used with the LA 48 positioned at 5.5 cm depth in water at isocentre.

The lack of peaks at -100, 0 and 100 mm in figure 5.8, indicated that the jaws were abutting completely.

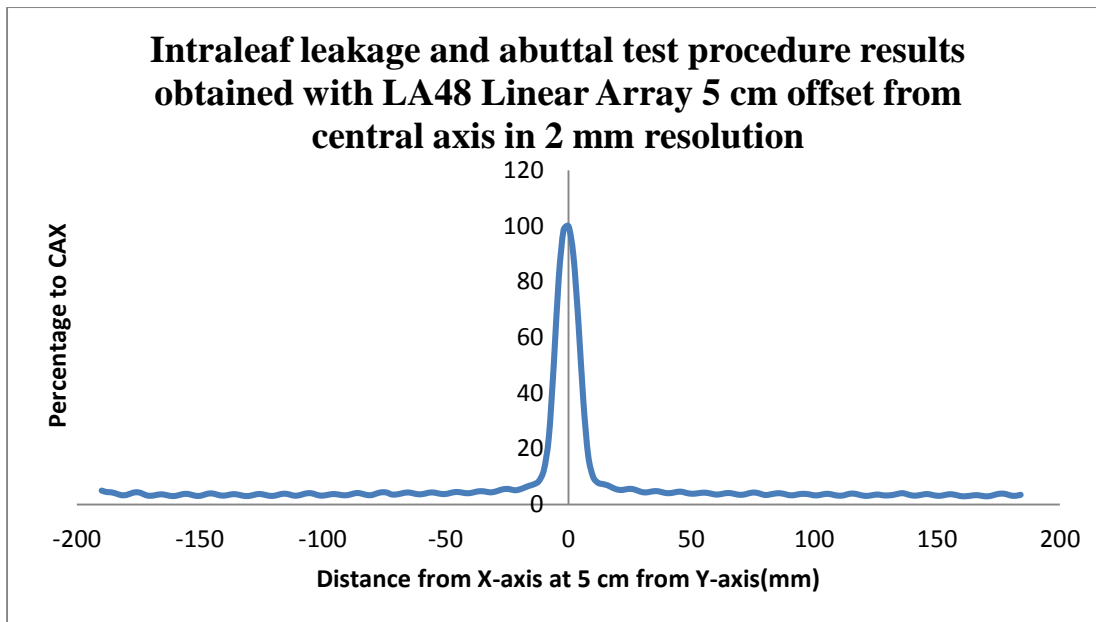
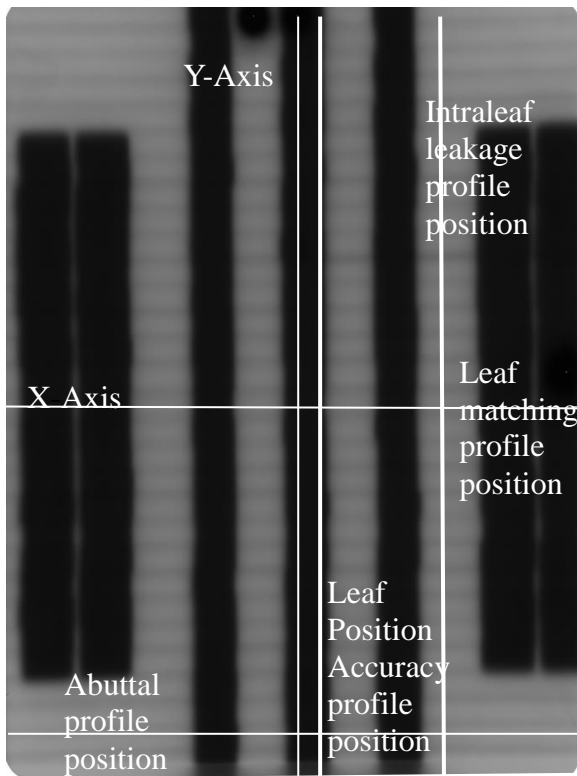


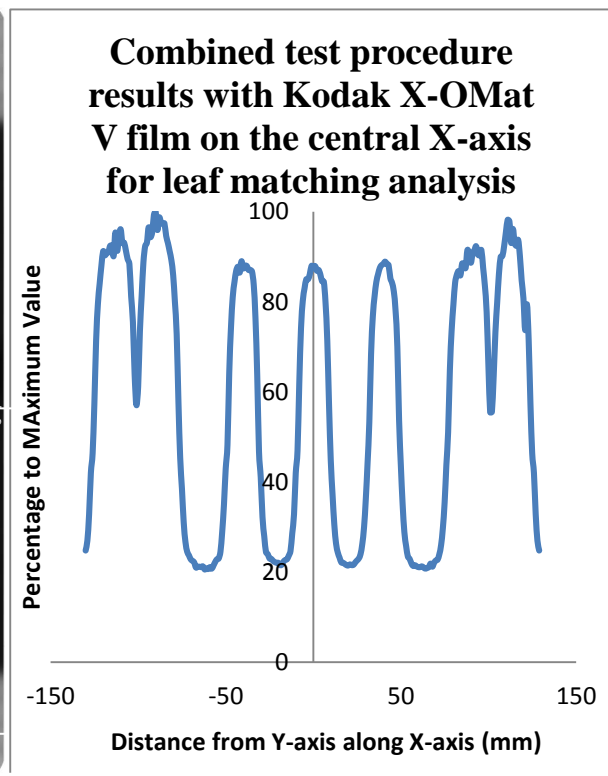
Figure 5.9: The LA 48 Linear array profile measured parallel to the Y axis and 5 cm offset from the central axis with a 2 mm resolution. The LA48 was positioned at 5.5 cm depth in water at isocentre.

The profile indicated that the transmission between the leaves (intraleaf leakage) were less than 5 % of the central axis dose.

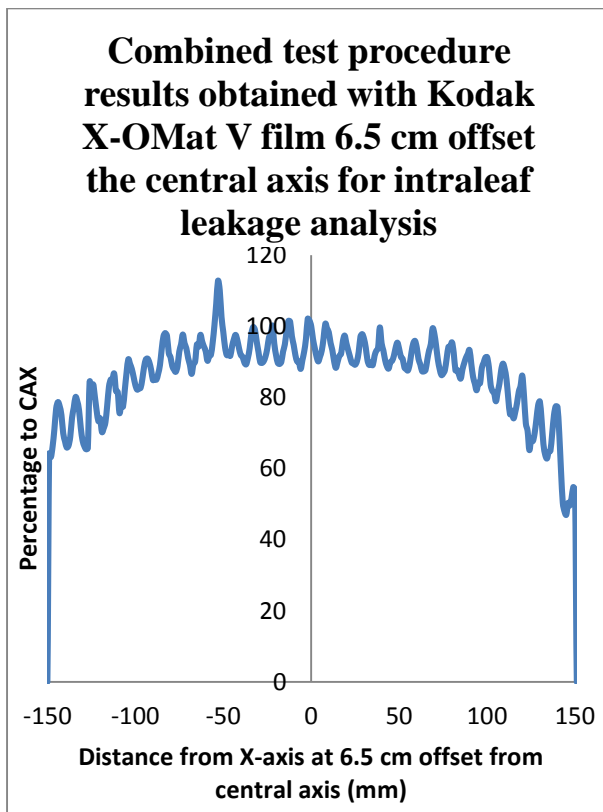
Combined test procedure



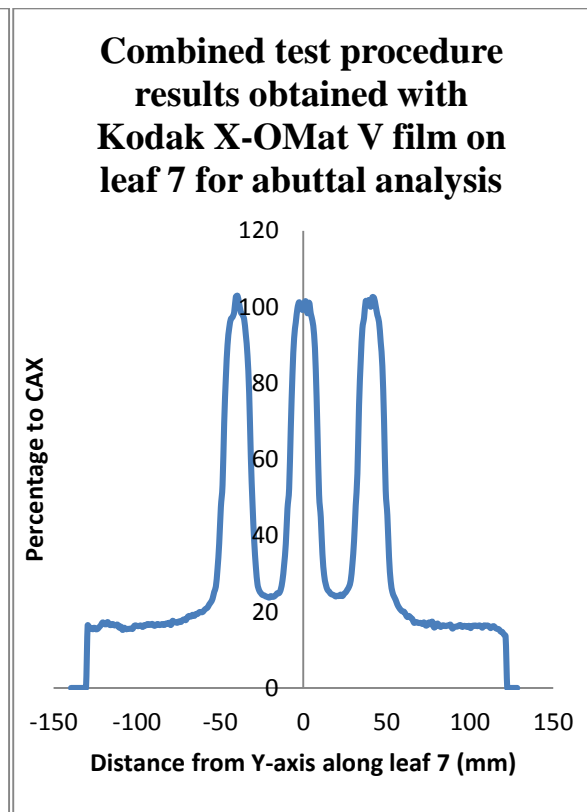
(a)



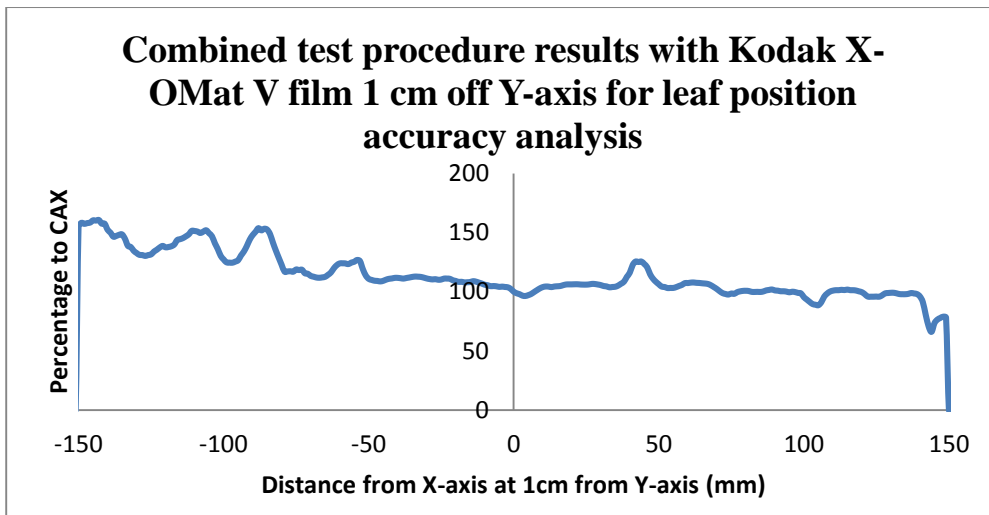
(b)



(c)



(d)



(e)

Figure 5.10: Image (a) is the Kodak X-OMat V film of the completed combined test procedure obtained using the UIP phantom with the film at isocentre with 30 MU per field segment. Graph (b) is the profile along the central X-axis for leaf matching analysis, graph (c) is the Y profile at 6.5 cm from the central axis for intraleaf leakage analysis, graph (d) is the profile of leaf 7 in the MLC for abuttal analysis and graph (e) is the profile 1 cm off the Y axis for leaf position accuracy analysis. These are all indicated on image (a) and the data were processed using the film calibration data and the MEPHYSTO software package.

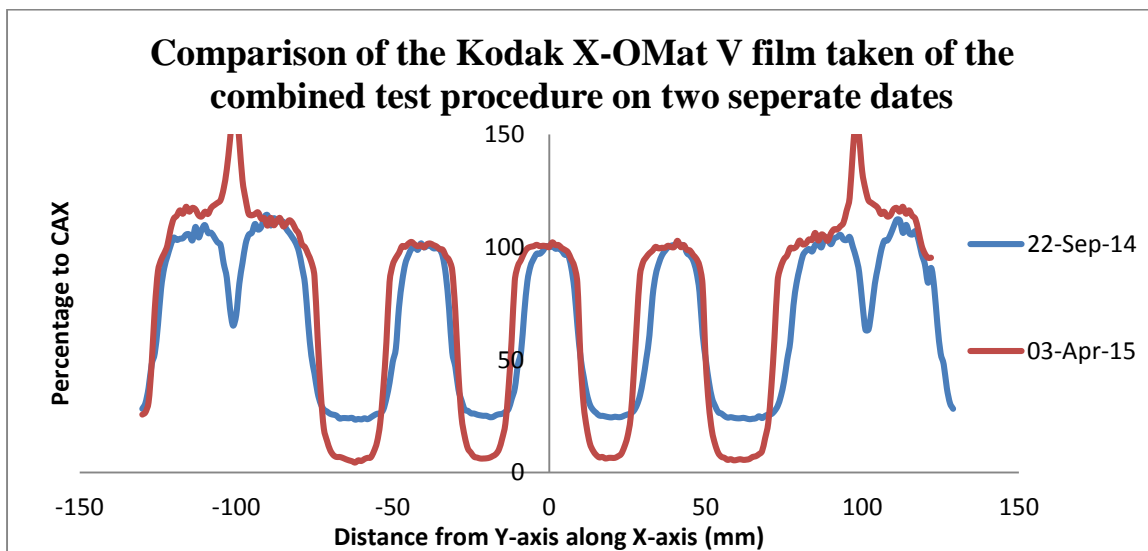


Figure 5.11: A comparison of the profile of the central X-axis produced from the Kodak X-OMat V film on the 22 September 2014 and the 03 April 2015.

The profiles in figure 5.11 were normalised to CAX and not maximum value as the rest of the matching procedure results for better profile analysis and visual comparison.

The profiles shown in figures 5.5 and 5.11 both showed troughs in the older data set and peaks in the newer set thus indicated that the combined test procedures produced the same results as the full leaf matching test procedure.

5.2 Results of the MLC Performance at LH

All results were carried out as set out in the methodology section and were obtained at LH on the Elekta Linac using 8 MV photon beam.

5.2.1 Calibration curves

As stated in section 5.2.1 calibration curves were specific for each portal imaging type, machine and energy used^{32, 33}. Figure 5.12(a) shows an example of one of the set of Gafchromic EBT2 films obtained for the purpose of the development of the calibration curve. The curve obtained from this set of films, graph 5.12(b), is inverted when compared to the other calibration curves produced (figure 5.2 and 5.13). The inversion is due to the MEPHYSTO software converting the true colour of the Gafchromic EBT2 film to black for processing and analysis. Figure 5.13 shows the calibration curve obtained for the Kodak X-OMat V film.

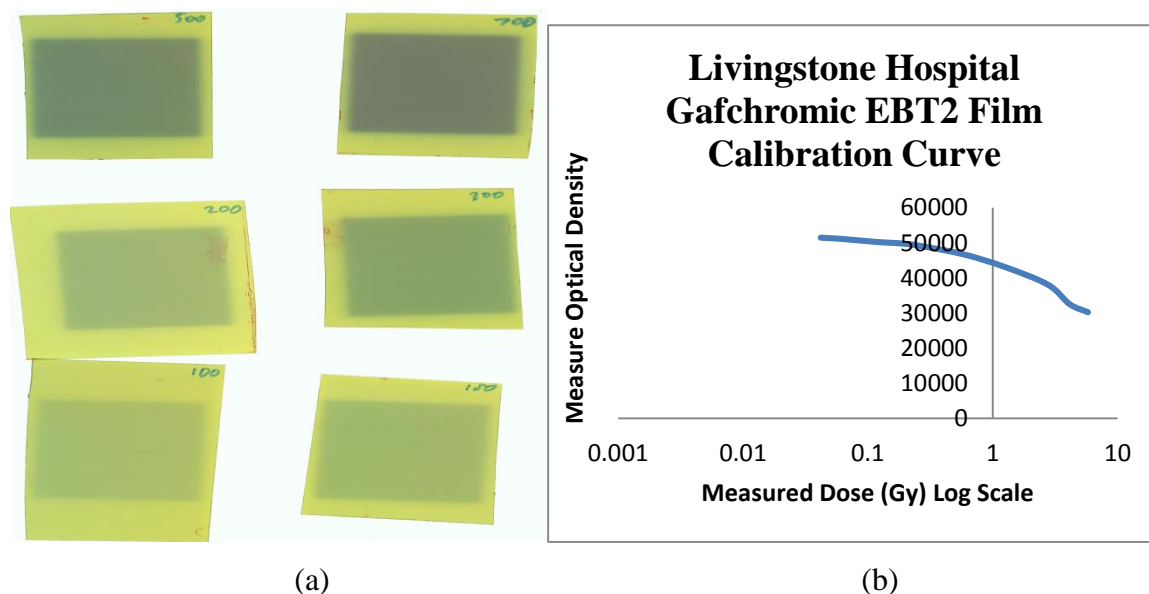


Figure 5.12: Image (a) is one of the sets of the Gafchromic EBT2 calibration films for LH 8 MV photon beam obtained by cutting the Gafchromic EBT2 into 9 x 10 cm² pieces and

exposing to increasing MU. Graph (b) is the linear-logarithmic curve obtained when plotting the measured optical density against the known dose for the corresponding MU field.

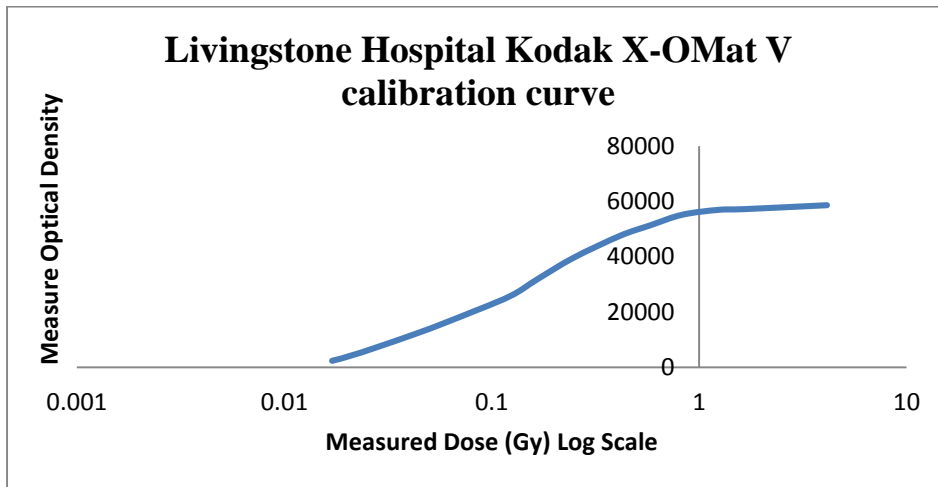


Figure 5.13: Kodak X-OMat V calibration curve for LH 8 MV photon beam obtained by plotting known dose points on calibration films to measured optical density at the same points on the scanned film on a linear-logarithmic scale.

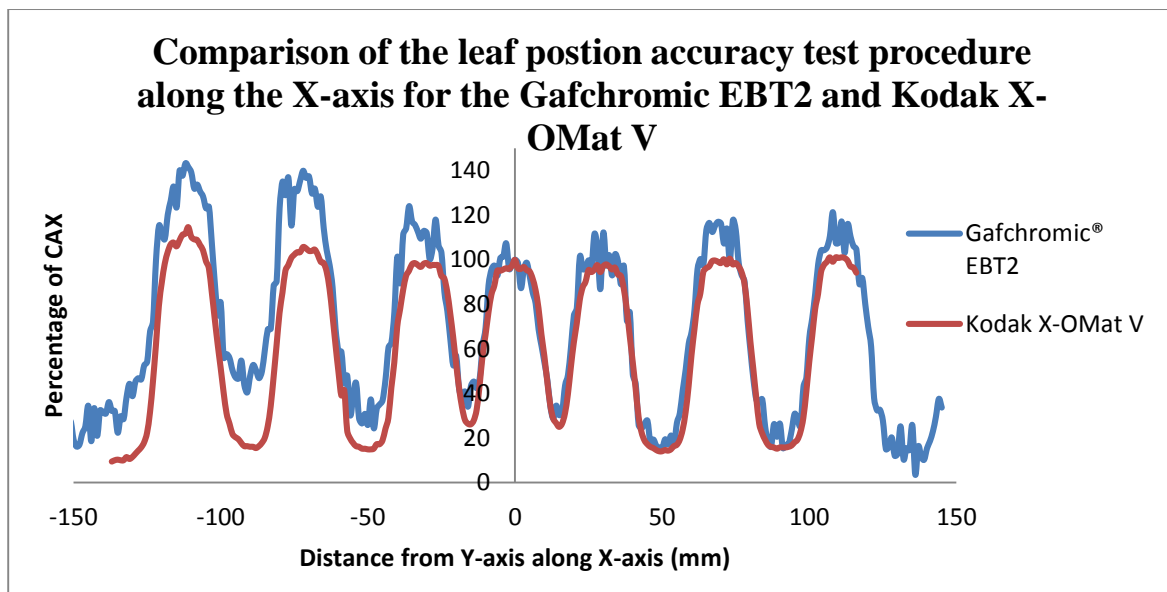


Figure 5.14: A comparison of the leaf position accuracy test procedure along the X-axis profile obtained with Gafchromic EBT2 and Kodak X-OMat V films.

As shown even though the film images of the Gafchromic EBT2 were inverted by MEPHYSTO, the profiles still demonstrated the same trend and have peaks at the expected positions. Thus, the resultant data were not affected by the inversion.

The EPID dose linearity curve was obtained with the EPID at its fixed SID of 160 cm and thus differs from the set up conditions of the other portal image devices used. In figure 5.15(a) an example of an EPID image used to generate the calibration is given. Figure 5.15(b) is the calibration curve generated for the EPID.

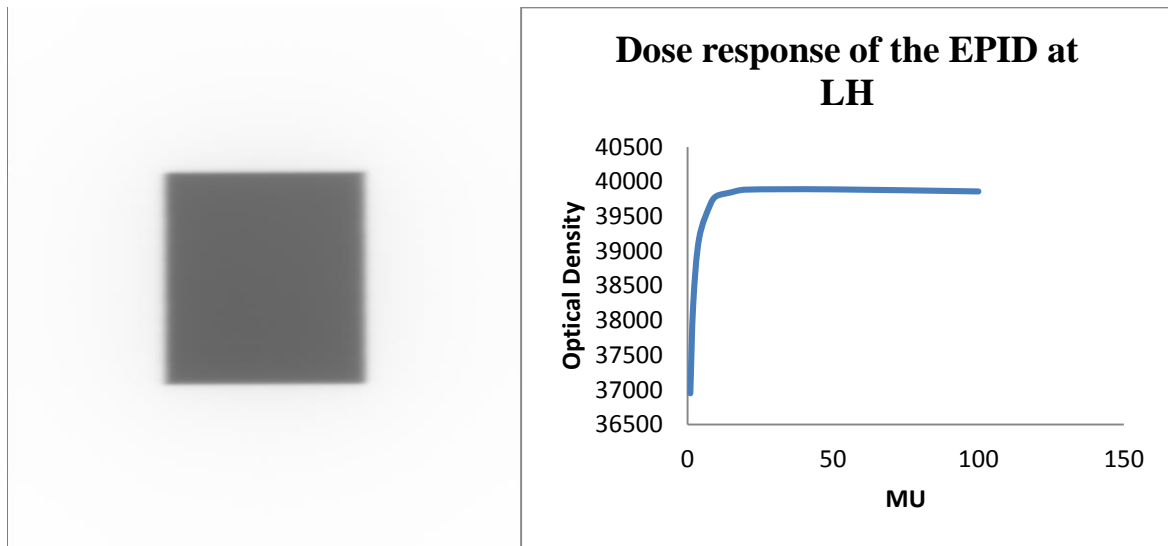


Figure 5.15: Image (a) is a sample of the images used to generate the EPID dose response for the LH 8 MV photon beam. Graph (b) is the EPID dose response curve obtained.

5.2.2 Quality Assurance test procedure results

An example of the planar output obtained for each test procedure and a corresponding profile are shown in figures 5.16 – 5.24.

Leaf matching test procedure

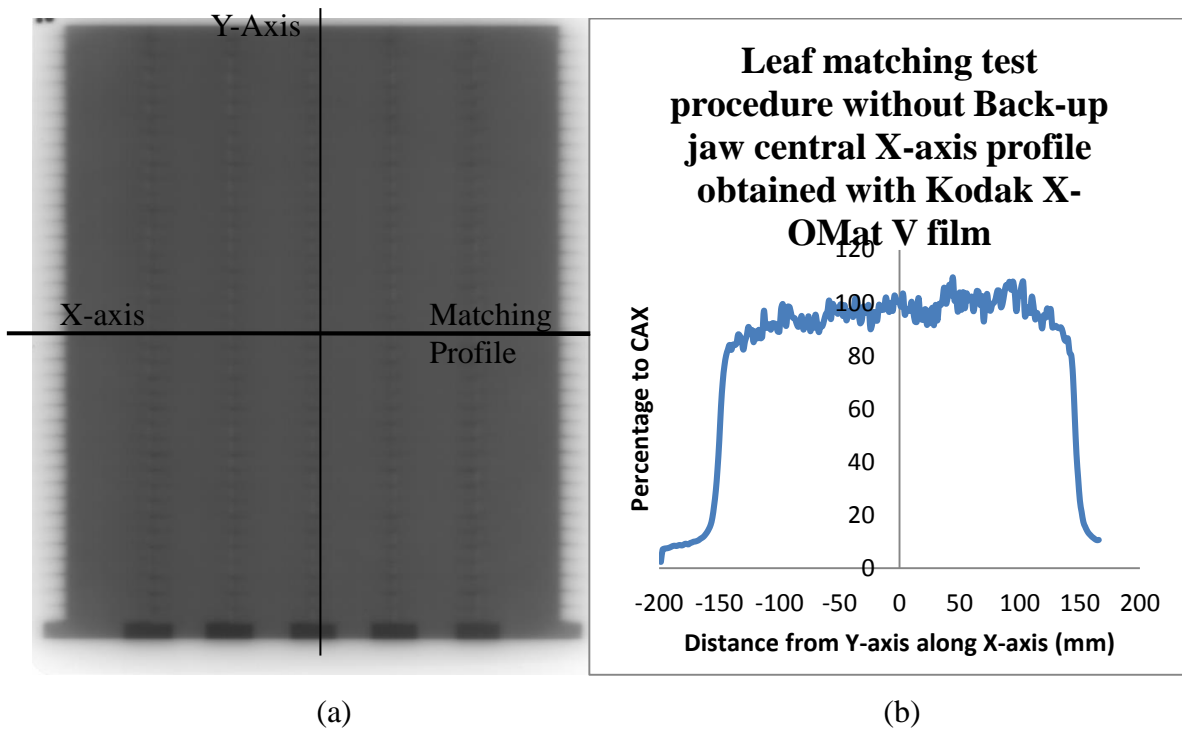


Figure 5.16: Image (a) is the Kodak X-OMat V film of the completed leaf matching test procedure (without back up jaws) in a field obtained using a polystyrene phantom. The film was placed at 5 cm depth in the phantom with an SSD of 63 cm and 30 MU per field segment was delivered. Graph (b) is the profile of the central X-axis as indicated on image (a). The data were obtained using the film calibration data, the MEPHYSTO software and adjusted to the field dimensions at isocentre.

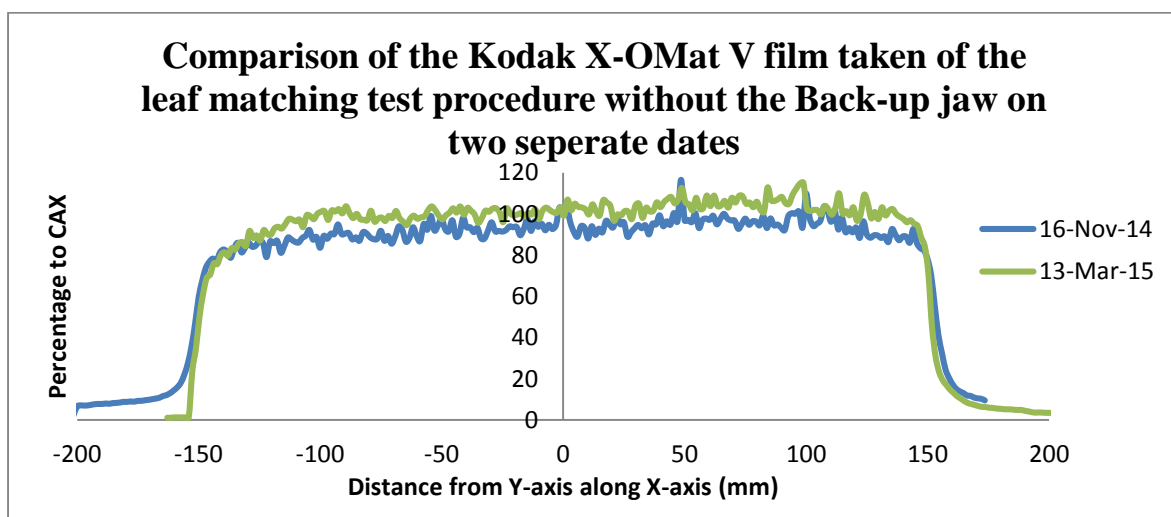


Figure 5.17: A comparison of the profile without the back-up jaw in the field along the central X-axis produced from the Kodak X-OMat V film on the 16 November 2014 and the 13 March 2015.

Both data sets in figure 5.17 had the same trend as well as showing no under- or over-travel of the leaves.

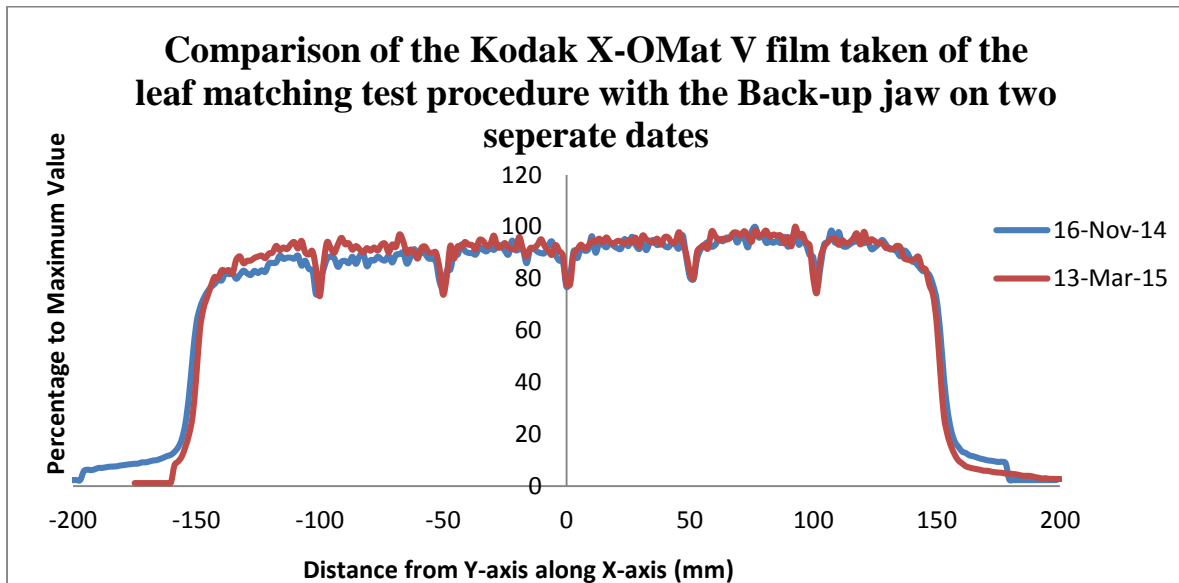


Figure 5.18: A comparison of the profile with the back-up jaw in the field along the central X-axis produced from the Kodak X-OMat V film on the 16 November 2014 and the 13 March 2015.

In figure 5.18 the dips at the field segment edges were due to the possible over-travelling of the MLC ahead of the back-up jaw

Leaf position accuracy test procedure

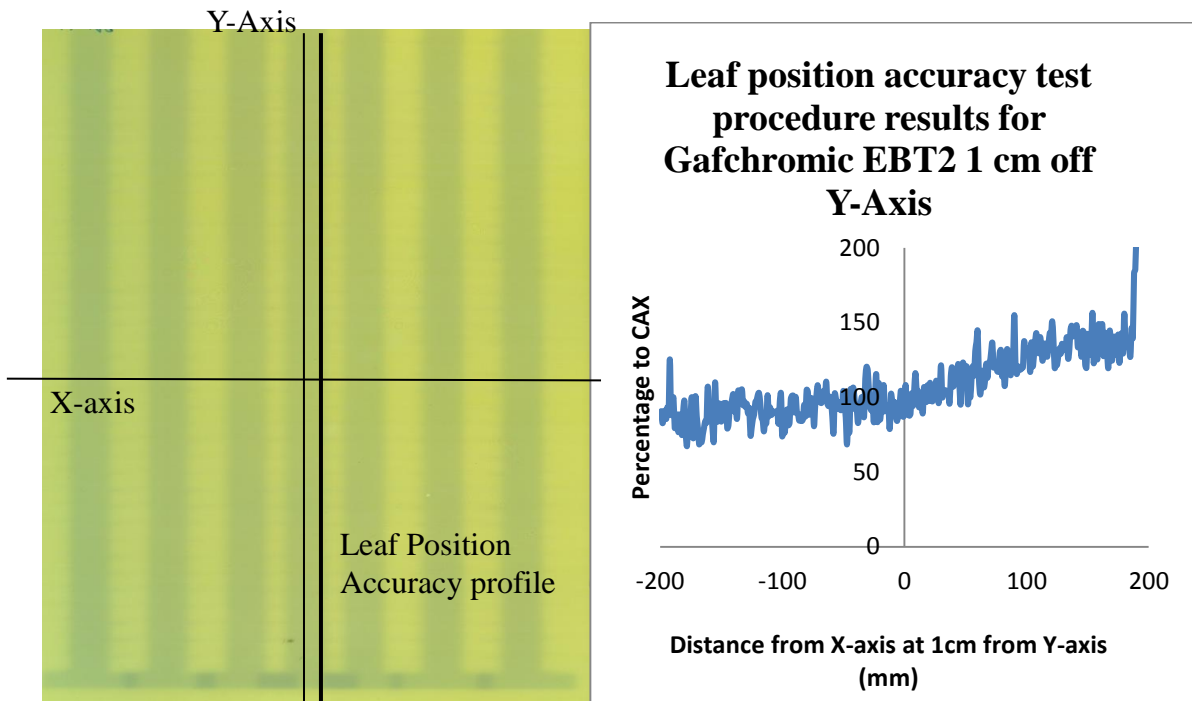


Figure 5.19: Image (a) is the Gafchromic EBT2 film of the completed leaf position accuracy test procedure obtained using a depth of 5 cm in a 7 cm thick polystyrene phantom with the film at isocentre using 80 MU per field segment. Graph (b) is the profile of the edge of the field defined by the MLC for the central field segment as indicated on image (a) obtained using the calibration film data and the MEPHYSTO software.

In figure 5.19(b), a peak would indicate that the leaf is further back than the leaf 20 position and a trough would indicate that the leaf is further forward. The image indicated that leaves 1-19 were closer in position to leaf 20 and that leaf 21 – 40 were progressively aligned further away from leaf 20.

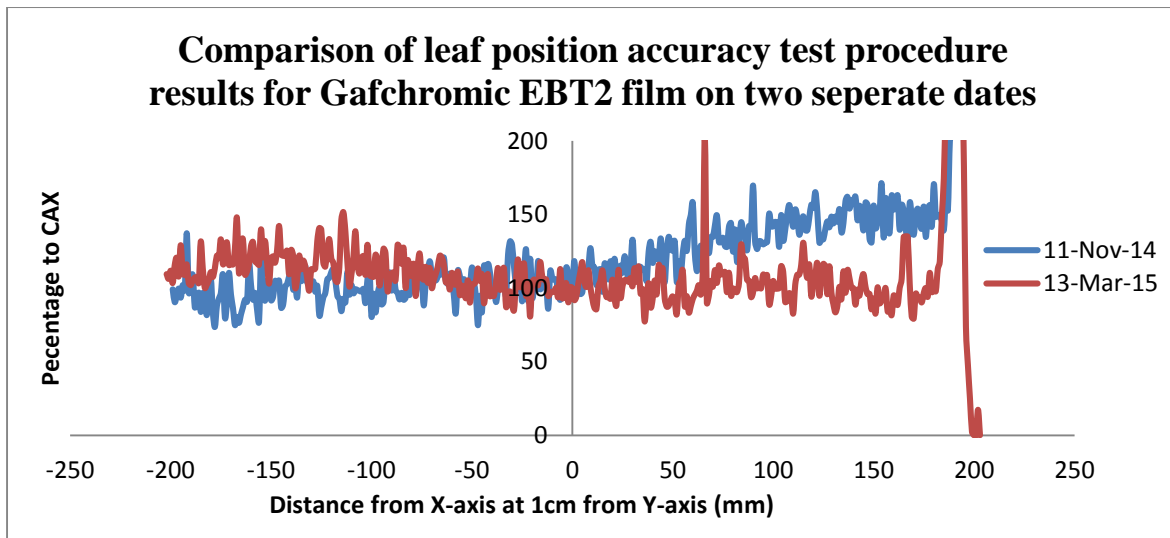


Figure 5.20: A comparison of the profile 1 cm off the Y-axis produced from the Gafchromic EBT2 film on the 11 November 2014 and the 13 March 2015.

In these profiles of figure 5.20, the newer data indicated that leaves in the negative axis direction were further back than leaf 20 and the leaves in the positive axis direction were closer to leaf 20. All the leaves were closer to leaf 20 for the newer profile as the older profile had a much larger variation in the percentage to CAX.

Intraleaf leakage test procedure

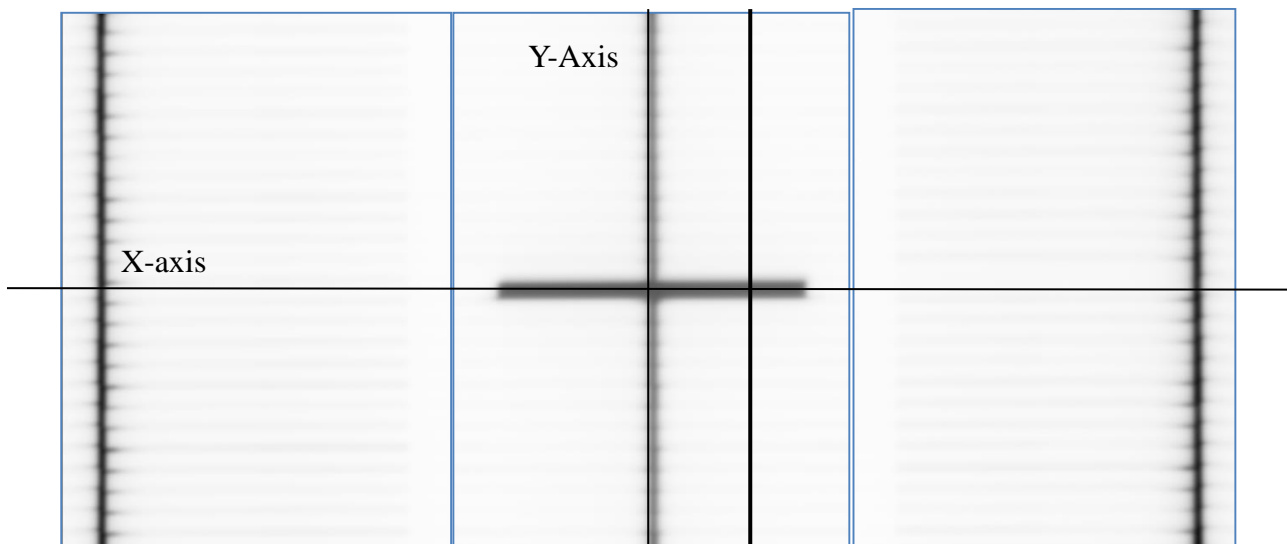


Figure 5.21: The three EPID images required to produce the intraleaf leakage test procedure. The EPID is at the fixed distance of 160 cm with no phantom in the beam line. The three images were calibrated and the profile required taken from each EPID image and summed.

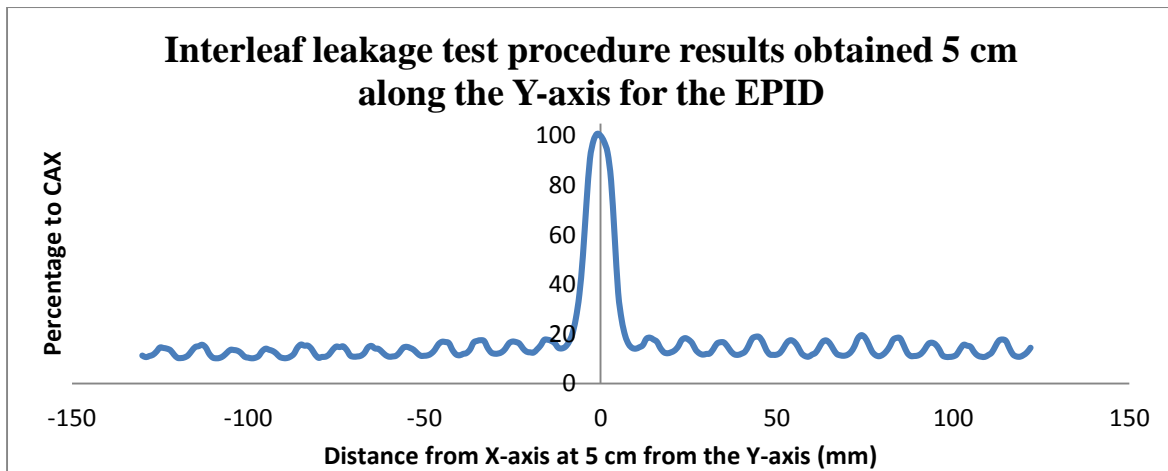


Figure 5.22: The EPID profile of 5 cm along the Y-axis for the intraleaf leakage and abuttal test procedure. The central peak is from leaf pair 20 which was open during the exposure.

The smaller peaks in figure 5.22 corresponded to the leakage between the edges of adjoining leaves. The doses were in the region of 15 – 20% of the maximum central dose but this was due to the back-up jaw of the MLC system being removed during the imaging of the test procedure.

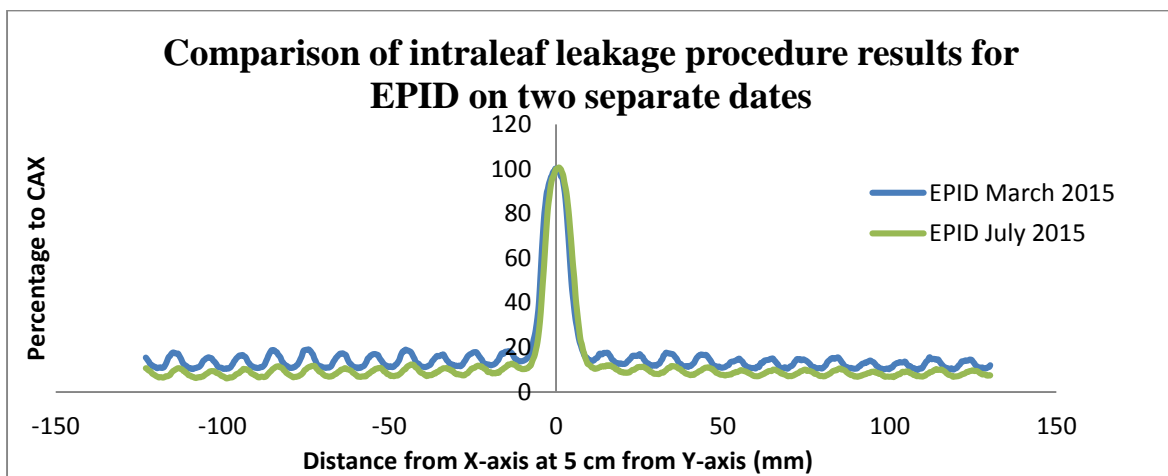
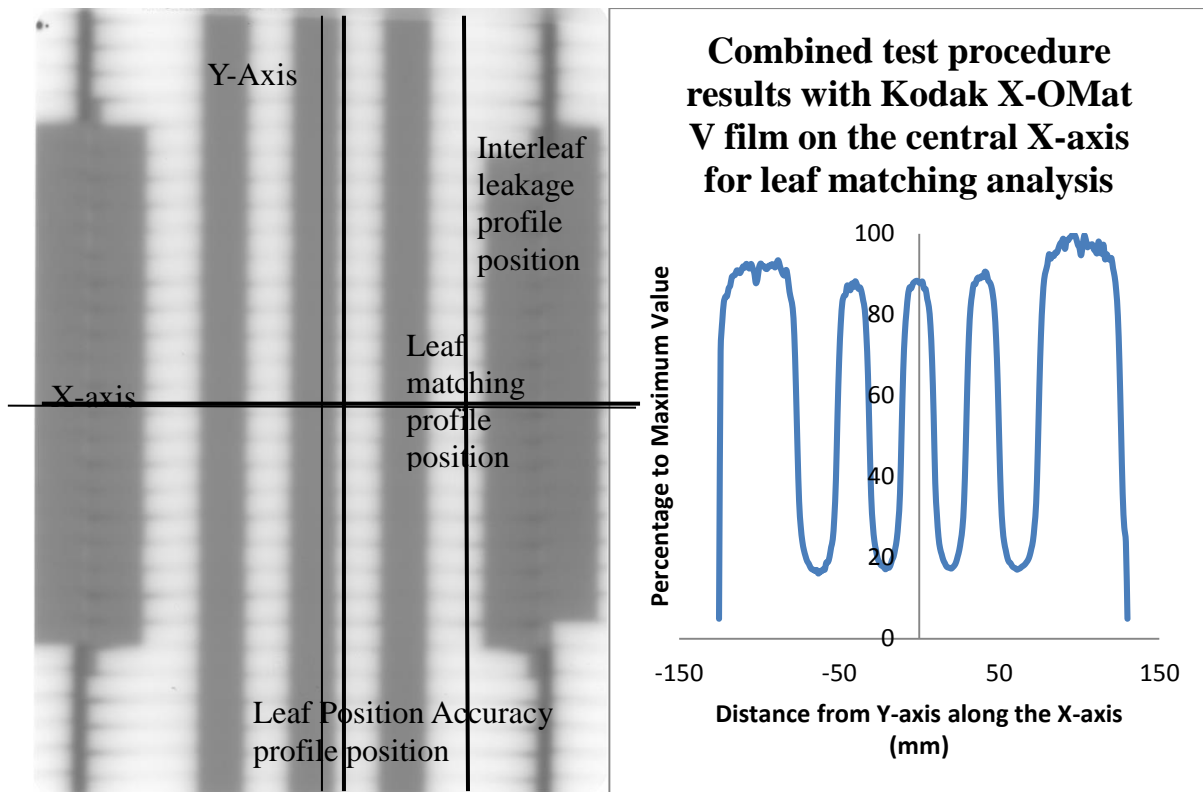


Figure 5.23: Comparison of the intraleaf leakage profile for the EPID taken at two different times

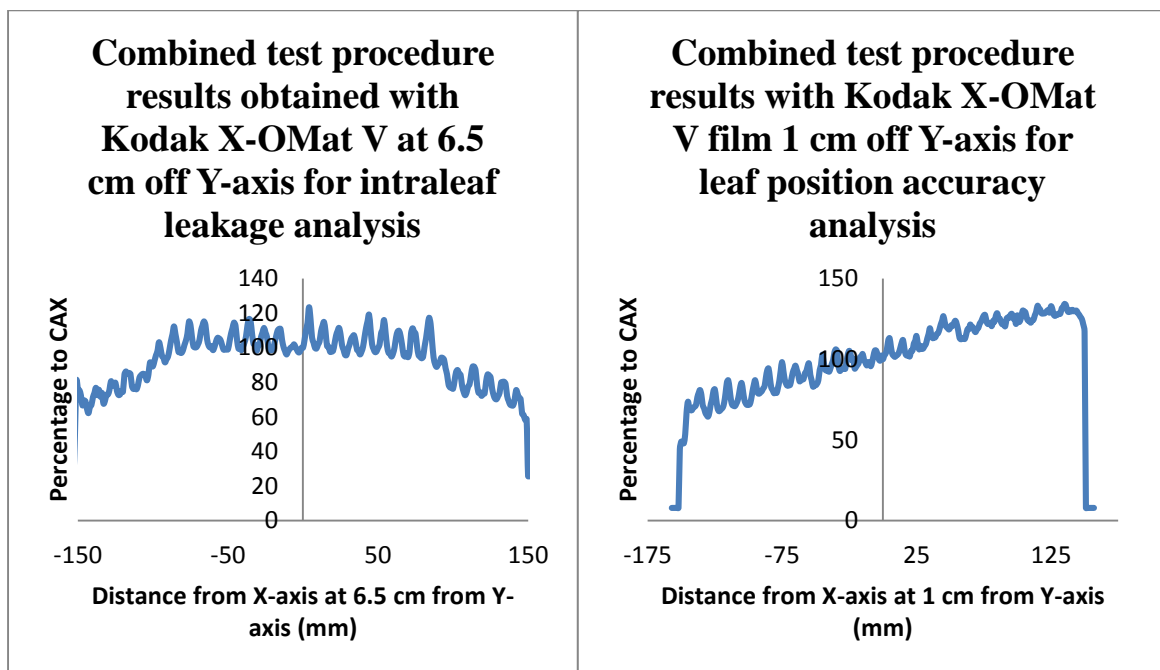
The difference in the profiles seen in figure 5.23 was due to a mirror replacement. The replacement of the mirror resulted in the projection of the light field changing.

Combined test procedure



(a)

(b)



(c)

(d)

Figure 5.24: Image (a) is the Kodak X-OMat V film of the completed combined test procedure obtained at 5 cm depth in a 7 cm thick polystyrene phantom at isocentre with each segment delivering 30 MU. Graph (b) is the profile of the central X-axis representing the leaf matching test procedure. Graph (c) is the profile of 6.5 cm off the Y-axis representing the

intraleaf leakage test procedure and graph (d) is 1 cm off the Y-axis for performing the leaf position accuracy test procedure. The profiles are indicated in image (a) and the analysis was obtained using the film calibration data and the MEPHYSTO software package.

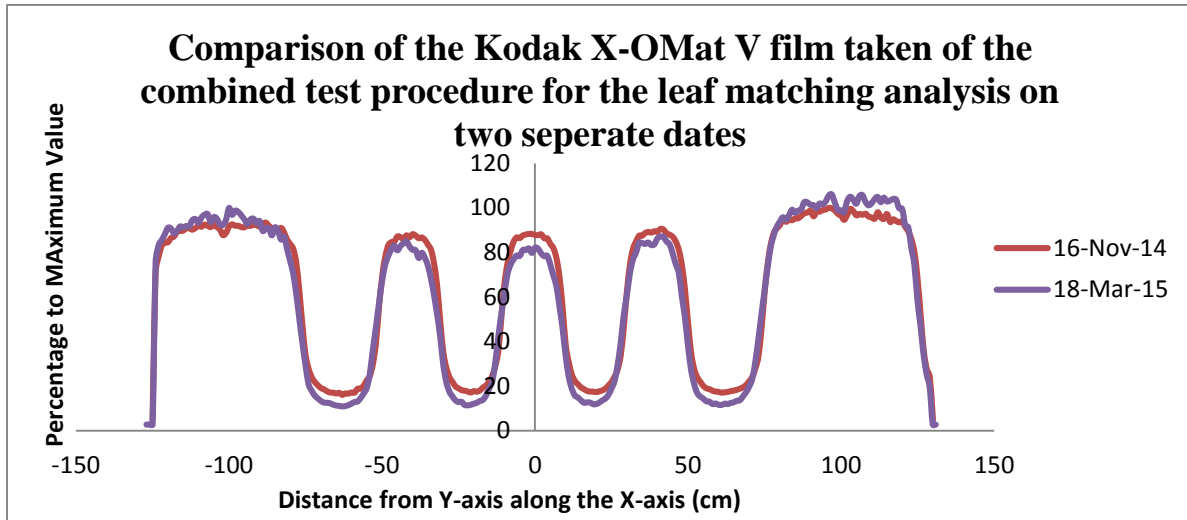


Figure 5.25: A comparison of the profile of the central X-axis produced from the Kodak X-OMat V film on the 16 November and the 18 March 2015 with 100% defined as maximum value for each profile.

5.3 CMJAH and LH Results Comparison

The figure (5.26 – 5.29) below are a comparison for each of the test procedures for the different centers in the study.

5.3.1 Leaf matching test procedure

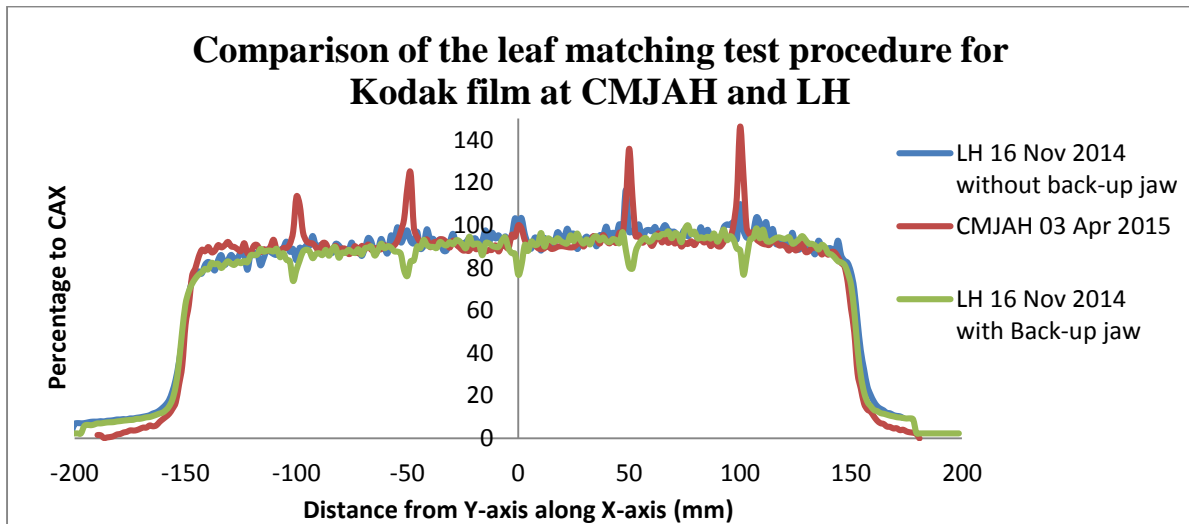


Figure 5.26: The comparison of the leaf matching test procedure at CMJAH and LH using Kodak X-OMat V film.

5.3.2 Leaf position accuracy test procedure

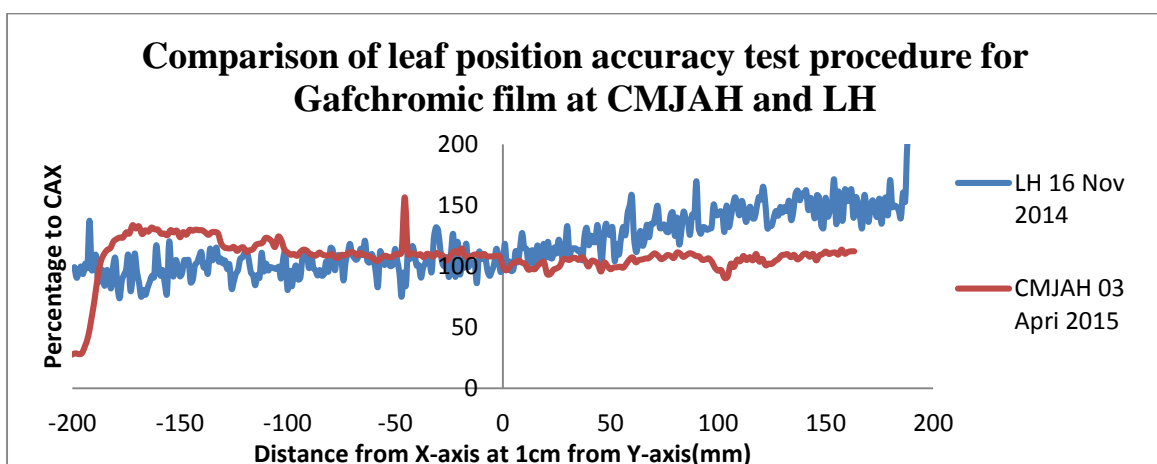


Figure 5.27: The comparison of the leaf position accuracy test procedure for CMJAH and LH exposed on Gafchromic EBT2 film.

5.3.3 Intraleaf leakage and abuttal test procedures

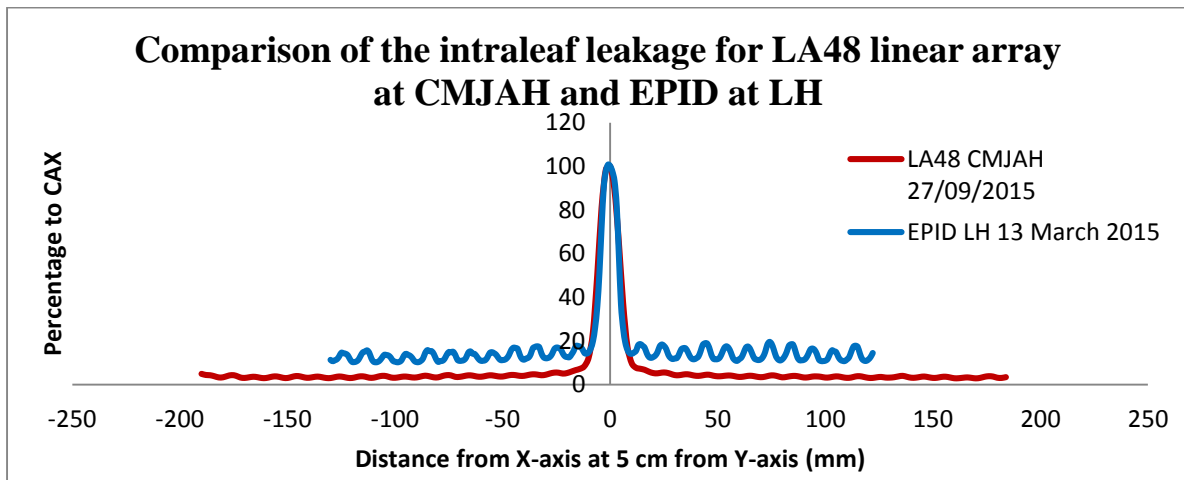


Figure 5.28: The comparison of the intraleaf leakage test procedure result from the LA 48 linear array (in water) at CMJAH and the EPID at LH (in air).

The LH MLC jaws do not abut but require a minimum separation distance of 5 mm and back-up jaws to close the field. Hence an abuttal profile for the LH MLC was not possible and a direct comparison with the performance of the CMJAH MLC could not be carried out.

5.3.4 Combined test procedure

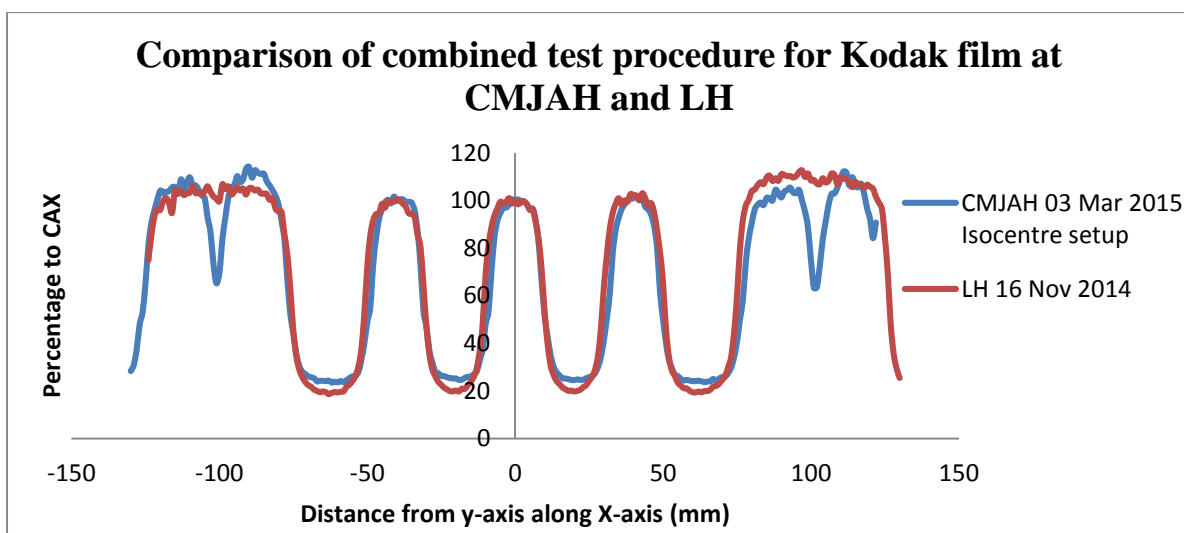


Figure 5.29: The comparison of the combined test procedure for CMJAH and LH exposed on Kodak X-OMat V film.

5.4 Portal Imaging Device and Linear Array Observations

Each of the portal imaging devices and the LA48 were capable of producing the similar results for the test procedures as shown in figure 5.30 for CMJAH and figure 5.31 for LH below. Each imaging type had its own set of unique limitations when it came to obtaining the results required.

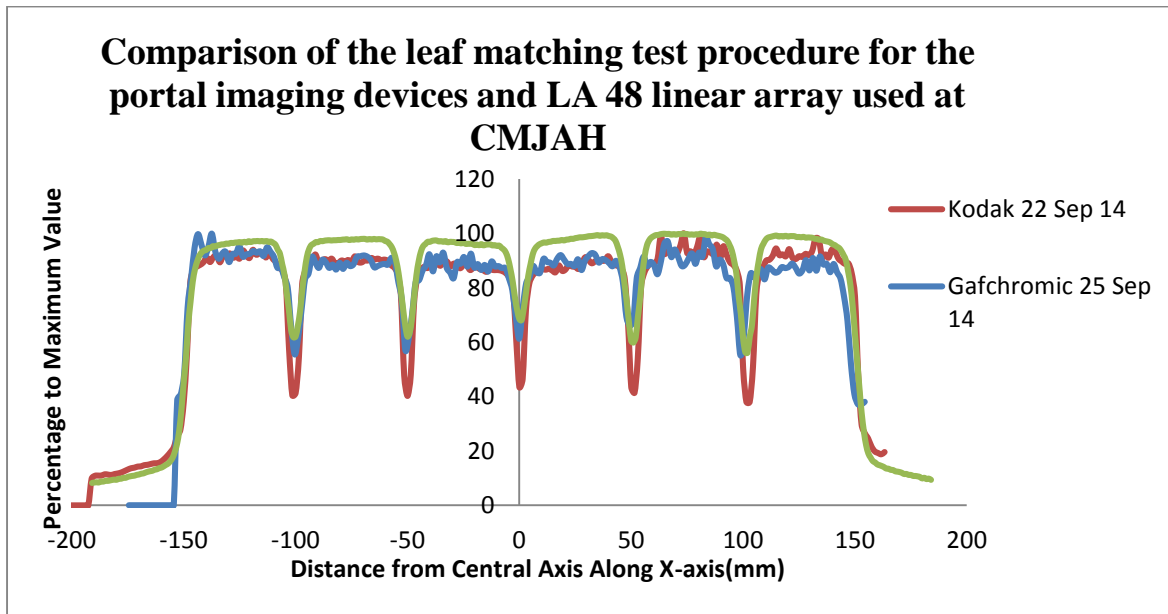


Figure 5.30: The comparison of the leaf matching test procedure for the portal imaging devices (Kodak X-OMat V and Gafchromic EBT2 films) and the LA48 linear array used at CMJAH.

The troughs and the peaks all matched in figure 5.30 with the only discrepancy being the height of the peaks and the depth of the trough. The Kodak X-OMat V film had a higher sensitivity and the best resolution at the lower dose areas thus the deeper troughs.

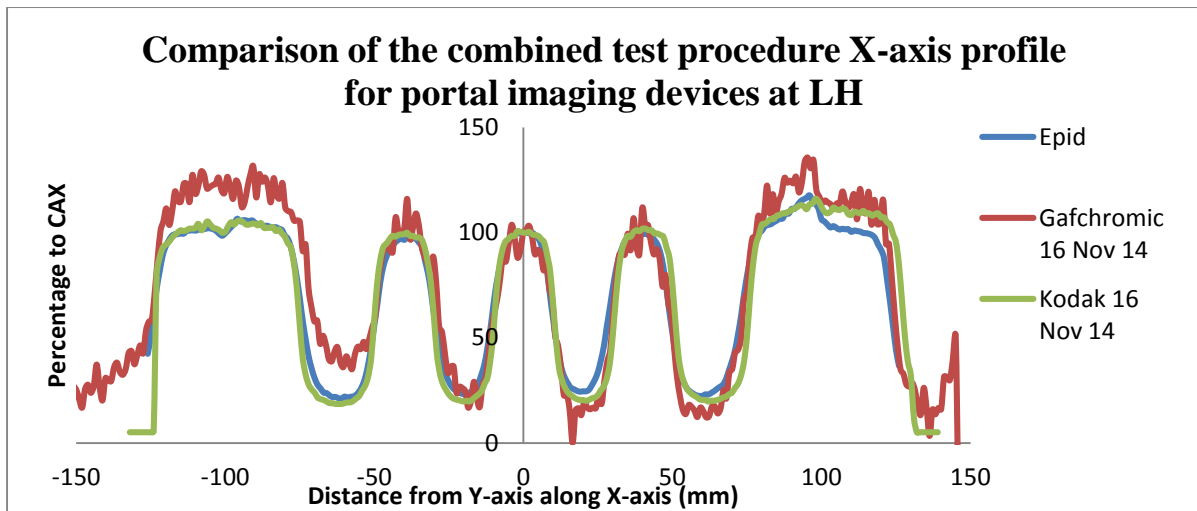


Figure 5.31: The comparison of the combined test procedure X-axis profile for the portal imaging devices (Kodak X-OMat V, Gafchromic EBT2 films and EPID) used at LH.

As in figure 5.30 the troughs and the peaks all matched in figure 5.31 with the only discrepancy being the height of the peaks once again.

5.4.1 Processing and Analysis Assessment of Imaging Devices

The imaging devices used, all had specific limitations and advantages for the dose range covered by the results of this study. Table 5.1 ranks the imaging devices according to the average exposure time which indicates how much Linac time would be required to obtain the results for the test procedures.

Table 5.1: The imaging devices used, ranked from the shortest average exposure time needed on the Linac to obtain the test procedure results

Rank	Imaging Device
1 st	EPID
2 nd	Kodak
3 rd	Gafchromic
4 th	LA 48

The exposure time is linked to the number of MU required by each imaging device as discussed in chapter 3.

The limitations of the radiographic Kodak film were that it required wet processing which was not readily available and had a long processing time. The other imaging devices did not require any processing. The Kodak film though had the highest sensitivity and best dose response for the portal image devices in the dose range investigated in this thesis.

The Gafchromic EBT2 film did not require any post irradiation processing as per the Kodak film however it was recommended that the Gafchromic film is only read or scanned 24 hours after exposure for image stability³³. This was done for this study but is not recommended if analysis and adjustment of MLC is needed urgently. The Gafchromic film showed a low sensitivity in the low dose range required for this study and produced profiles which are distorted and not as smooth as obtained with the other imaging devices. Thus the validity of the results obtained with the Gafchromic film can be brought into question.

The LH EPID system is ranked as having the shortest exposure time but was only able to obtain images of one field segment per exposure. This slowed the total exposure, capture and analysis as the segments had to be recombined to obtain a completed test procedure image. The detector field size of 26 x 26 cm² also affected the results of certain tests (leaf matching) and limits the maximum field size that could be tested.

The LA48 required set up in a water tank before any exposure can be done. This was very time consuming when compared to the portal imaging devices. It did however produced the best quality of profiles as it was a directly calibrated measurement in real time with no additional processing of device or data required.

6. ANALYSIS

6.1 Introduction

The analysis of the QC procedures was conducted based on the tolerance level set out in AAPM TG142 ‘Quality assurance of Medical Accelerators’⁹ and the 2013 CPQR ‘Medical Linear Accelerators and Multileaf Collimators’¹⁰. Further analysis was done to determine the reproducibility and compatibility across the different Linac platforms and imaging devices used. Table 6.1 below details the different tolerance levels stated and the baseline is chosen to be the Kodak film at each institution. The procedures listed in the two guidance documents do not necessarily have the same names but the appropriate procedure tolerances were used.

Table 6.1: Tolerance values according to AAPM TG 142 and CPQR 2013 for the test procedures conducted on the CMJAH and LH Linac systems.

Procedure	AAPM TG142 Tolerance	CPQR Tolerance	Action
Leaf Matching	1 mm	1 mm	2 mm
Leaf Positioning Accuracy	1 mm	1 mm	2 mm
Intraleaf Leakage	0.5 % from baseline	2% from Baseline	3% from Baseline
Leaf Abuttal	0.5% from baseline	2% from Baseline	3% from Baseline

6.2 Leaf Matching Test Procedure Analysis

The ideal result for the leaf matching test procedure would be a smooth solid profile. The deviation from the smooth profile is expected at the matching points of the fields when there is under- or over-travel of the MLC. When this occurs there would be either spikes or dips in

the profile at distances of ± 100 , ± 50 and 0 mm from the central axis and at ± 100 mm from the central axis for the combined test procedure. If there were dips below the expected profile the field was smaller than the expected field size due to the under-travel of the MLC and a spike in the profile indicated that the field was larger than expected due to the over-travel of the MLC.

The design of the MLC system on the Elekta Linac used at LH was such that the leaf matching test procedure could be completed with the back-up jaws either in the field or out of the field. With the back-up jaws out of the field there were no significant spikes or dips corresponding to the field matching points as shown in figure 5.16(b). The fields were matching and thus the MLC leaves were moving to the same position. With the back-up jaws in the field, the MLC leaves defined the field edge closer to the CAX and the back-up jaw defined the field edge further from the CAX with the MLC leaves offset by 2 mm as designed. This was due to the back-up jaw travelling on a straight plane and the MLC leaves on an elliptical plane within the collimator head. Thus, the MLC leaves which were ahead of the back-up jaw would over-travel on the matching field edges creating dips on the field matching points due to a reduction in dose through the MLC leaves. Figure 6.1 shows an example of one of the leaf matching test procedure subfields with the outline defining the field set.

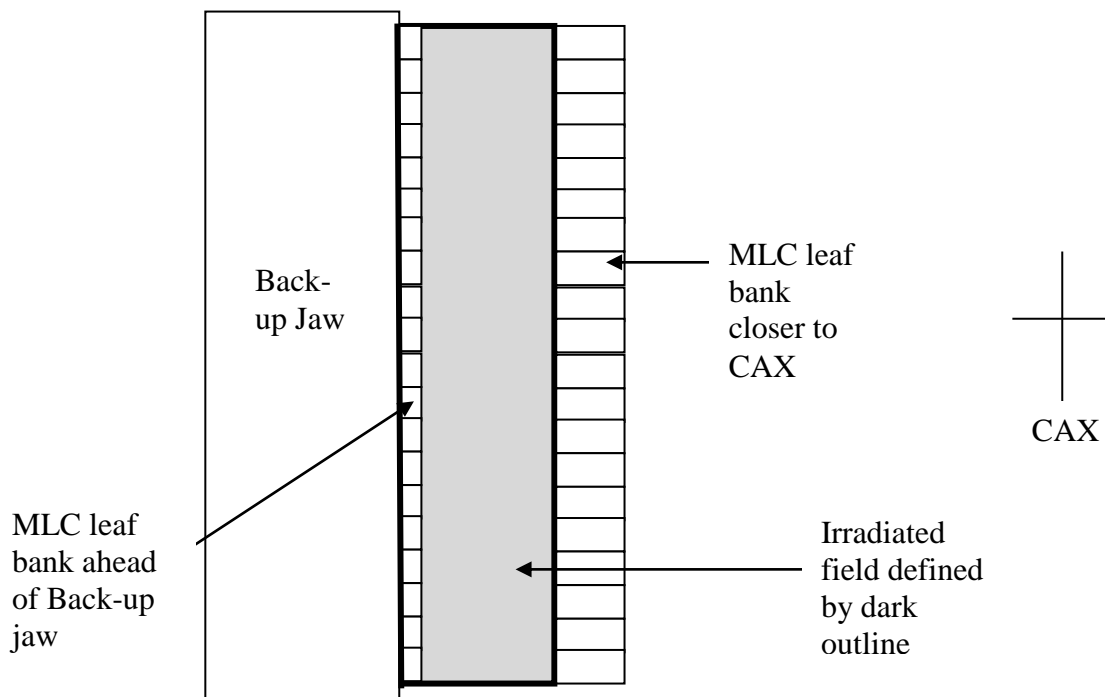


Figure 6.1: An example of a leaf matching test procedure subfield with the position of the backup jaw and MLC shown with respect to the irradiated field size.

For all leaf matching and combined test procedure profiles such as those shown in figures 5.5, 5.10(b), 5.11, 5.17, 5.18 and 5.24(b), the full widths half maximum (FWHM) were calculated and displayed in Table 6.2. The FWHM values give the distance between the jaw positions at 50% of the dose for the curve as seen in figure 6.2.

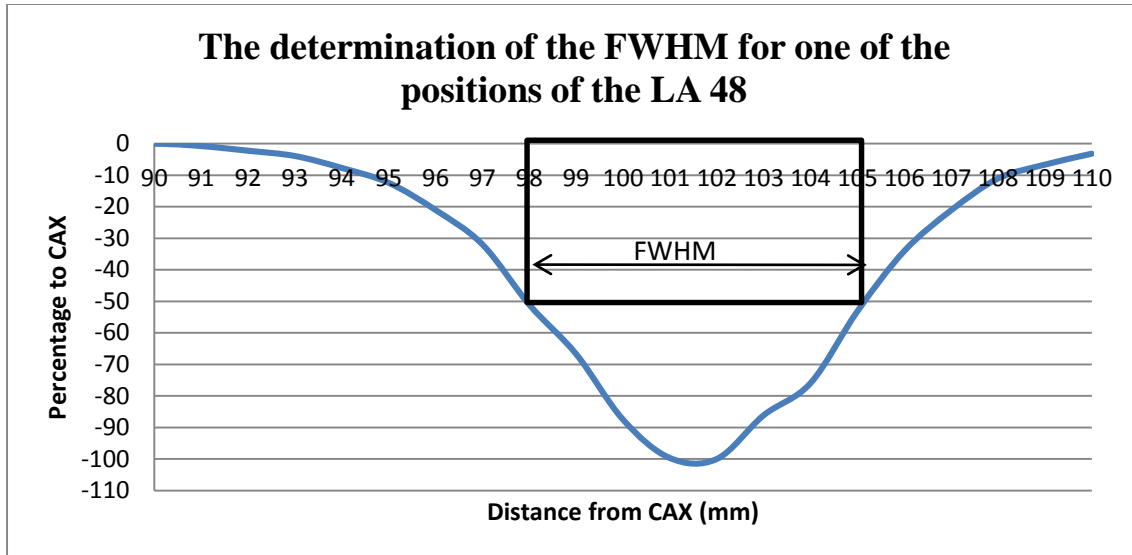


Figure 6.2: An example of the method used to determine the FWHM values for the matching data results. The curve shown is for the LA 48 detector at position 100 mm from CAX.

Table 6.2: The average FWHM for all leaf matching and combined test procedures for both CMJAH and LH for all imaging devices.

Imaging Device	CMJAH average FWHM (mm)	CMJAH combined average FWHM (mm)	LH average FWHM (mm)	LH combined average FWHM (mm)
LA 48 1	-6.8	-6.75	--	--
LA 48 2	-6.9	-6.5	--	--
Kodak 1	-5.2	-5.75	-3.9	-3.25
Kodak 2	3.5	4.13	-3.4	-3.63
Kodak 3	--	--	-3.75	-4.0
Gafchromic 1	-4.95	-5.25	--	-3.5
Gafchromic 2	8.35	7.63	--	-3.38
EPID 1	--	--	-5.25	-5.5
EPID 2	--	--	-5.7	--

The numbering of the imaging devices refers to the different time periods or SSD that the results were obtained on with a minimum time period of four months from the previous results.

The positive average FWHM denoted when the profiles had spikes and thus over-travel of the MLC was seen. The negative average FWHM denoted when the profiles had dips and thus an under-travel of the MLC was seen.

There was no constancy in the values obtained for the average FWHM values between the imaging devices. All the imaging devices at CMJAH showed the same result trend, which was, negative values for first result and positive for the second except LA 48 which were taken days apart. The change in the results was due to the MLC being recalibrated between the data sets.

The LA 48 average FWHM values were all within 0.5 mm but differed from the Kodak 1 and Gafchromic 1 values by up to 2 mm. The Gafchromic 2 average FWHM values were greater than those for the Kodak 2 by between 3 – 4 mm whereas the Gafchromic 1 and Kodak 1 values only differ by 0.3 - 0.5 mm. The reason that this result occurred was that the Gafchromic 2 profiles spikes were not as sharp or long as the Kodak profile spikes as seen in figure 6.3. When the spikes were re-normalised for determination of the average FWHM, the Gafchromic 2 results were much broader than the Kodak 2 results causing the discrepancy in the FWHM seen in table 6.2.

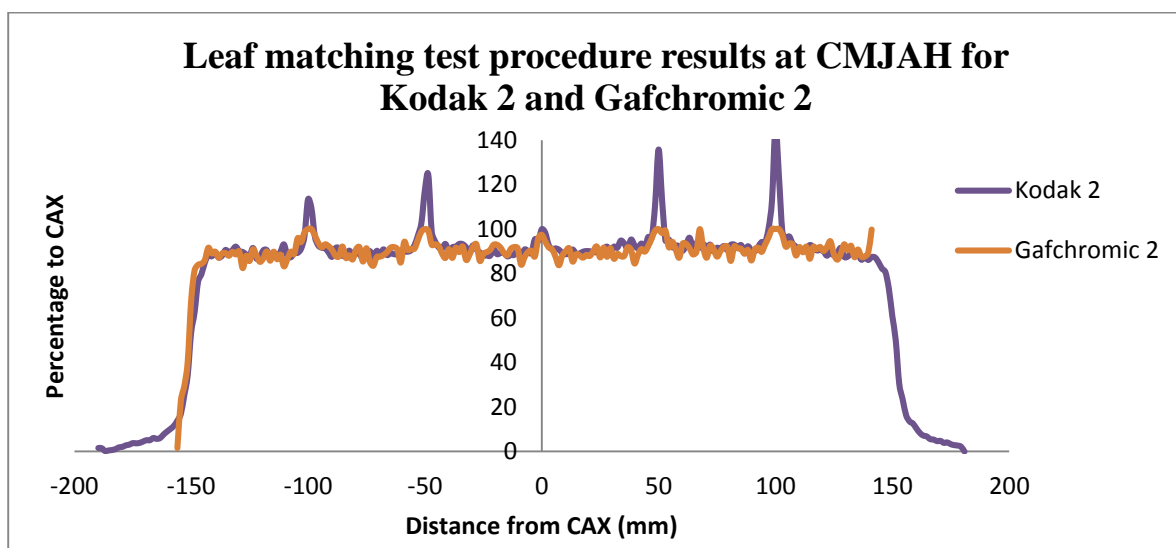


Figure 6.3: The leaf matching test procedure profiles for Kodak 2 and Gafchromic 2 showing the difference in the shape of the spikes at the matching positions.

Even though the MLC jaws positions tests and the average FWHM results indicated an inaccuracy in the jaw position. The tests performed in this thesis were unable to distinguish what the requirements were for any adjustments or suggested corrections to the leaf banks. This information could be obtained if the leaf matching test procedure was repeated with a collimator rotation of 180° . If the rotated subfields match then the MLC leaf banks were symmetric and further analysis on leaf bank movement could be done. Thus, a more in-depth study of the leaf matching test procedure is required to obtain a complete quantitative analysis of the MLC jaw matching.

The LH average FWHM values for the profiles with the back-up jaw in the field were measured and shown in table 6.2 but the jaws would not be adjusted as the fields without the back-up show that the MLC jaws match. All the Kodak and Gafchromic average FWHM values fall between 3.25 – 4.0 mm which was expected as the MLC leaves are offset 2 mm from the backup jaw into the field. Only one result was obtained from the EPID 1 data for the combine test procedure due to the edge of the field falling at the end of the detector. To accommodate the use of the EPID 1 data for the combined test procedure, the procedure can be redesigned moving the match point closer to CAX.

6.3 Leaf Position Accuracy Test Procedure Analysis

The ideal result of the leaf positioning accuracy procedure would be a straight profile with all leaves in line with the central MLC leaf pair (leaf 21 at CMJAH and leaf 20 at LH). The value corresponding to the centre of each leaf was obtained from the curves displayed in chapter 5. These data sets were then plotted with respect to the central leaves. This data indicated whether more or less dose was detected by the imaging device (and not the individual leaf positions) with respect to the central leaves. The inverse of the dose versus leaf number was plotted to show the actual leaf position with respect to the central leaf (figure 6.4).

In this configuration, if a leave had a value greater than the central leaf at 100 % then that leaf is further ahead of the central leaf and thus in the field. If a leave had a value smaller than the central leaf at 100% then the leaf lags the central leaf. From the plot it could be determined which leaves needed to be moved and in which direction. The adjustment of the leaf could then be done in conjunction with the visual light field display of the leaves at isocentre.

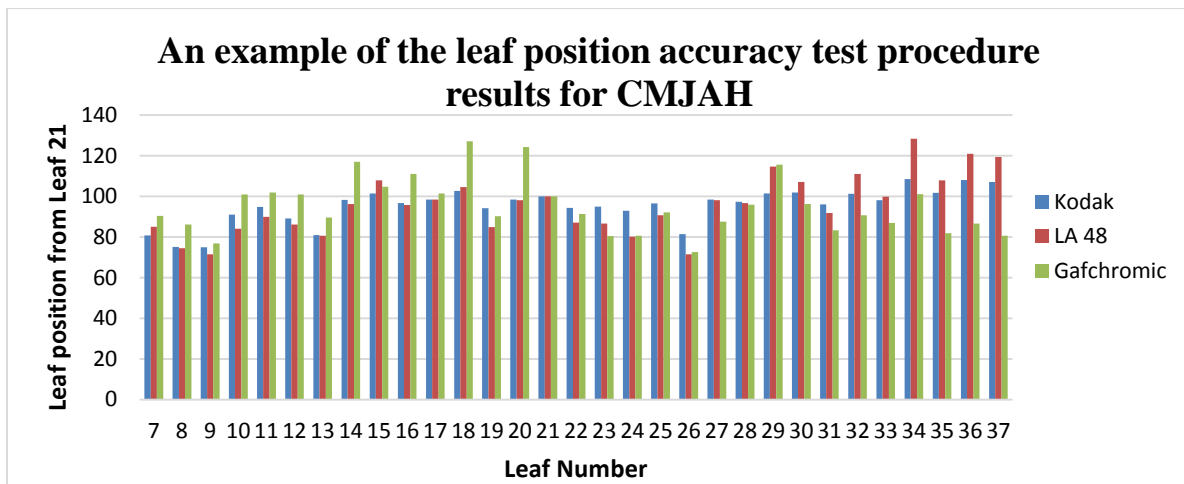


Figure 6.4: An example of the leaf position accuracy test procedure results for all imaging devices at CMJAH taken in September 2014 normalised to leaf 21 with leaves below 100% being out of the field and leaves above 100% being in the field.

Figure 6.4 shows that the Kodak 1 film and LA48 1 linear array are in better agreement than the Gafchromic 1 film which had a greater leaf position variation than the other imaging devices used.

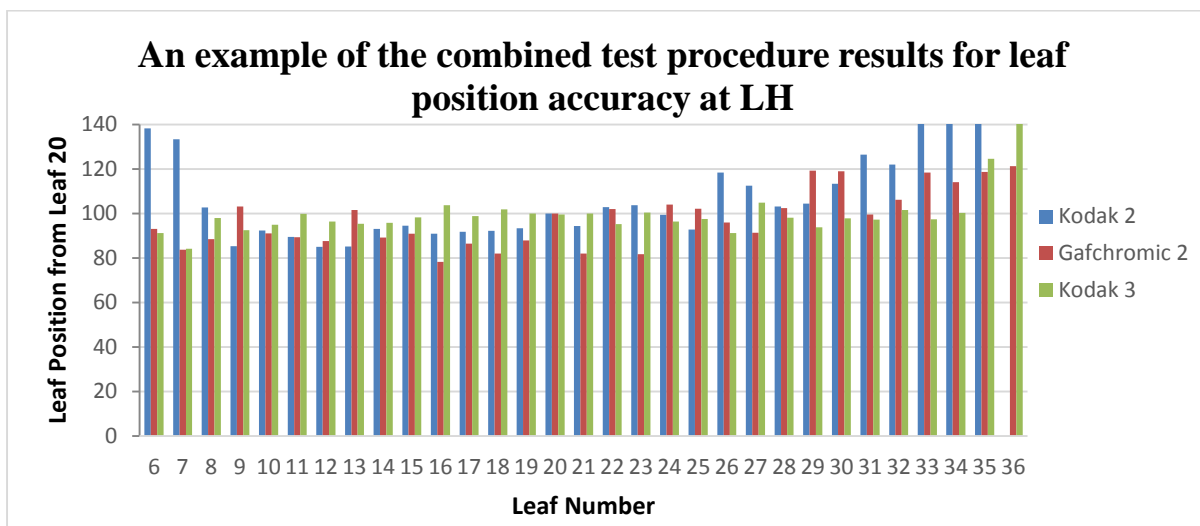


Figure 6.5: An example of the combined test procedure results for leaf position accuracy for Kodak and Gafchromic film at LH taken in March 2015 normalised to leaf 20 with leaves below 100% being out of the field and leaves above 100% being in the field.

Figure 6.5 shows that the Kodak 3 film and Gafchromic 2 film were in better agreement than the Kodak 2 film which had the same trend as the other imaging device but had larger

outlining values at both large and small leaf numbers.

The average leaf position was determined for both centres for all imaging devices and displayed below in table 6.3. How much the leaf positions vary from 100% (leaf 21 at CMJAH and leaf 20 at LH) were obtained from the deviation from the 100% information in table 6.4. Thus, the deviation values were not linked to the average leaf position values. The ideal values for the average leaf position should be 100% and the standard deviation from the central MLC leaf should be 0.

Table 6.3: The average leaf position for all leaf position accuracy and combined test procedures for both CMJAH and LH for all imaging devices.

Imaging Device	CMJAH average Leaf Position (%)	CMJAH combined average Leaf Position (%)	LH average Leaf Position (%)	LH combined average Leaf Position (%)
LA 48 1	95.84	--	--	--
LA 48 2	--	--	--	--
Kodak 1	95.40	88.68	100.17	100.28
Kodak 2	92.93	92.43	100.62	102.27
Kodak 3	--	88.69	96.39	97.33
Gafchromic 1	93.96	95.00	89.84	93.12
Gafchromic 2	92.10	89.69	98.39	96.50
EPID 1	--	--	100.72	102.22
EPID 2	--	--	99.69	101.16

Table 6.4: The deviation from 100% for CMJAH and LH for all leaf position accuracy and combined test procedures for all imaging devices where 100% corresponds to leaf 21 at CMJAH and leaf 20 at LH.

Imaging Device	CMJAH deviation from leaf 21 (%)	CMJAH combined deviation from leaf 21 (%)	LH deviation from leaf 20 (%)	LH combined deviation from leaf 20 (%)
LA 48 1	±14.38	--	--	--
LA 48 2	--	--	--	--
Kodak 1	±9.76	±16.43	±10.26	±16.24
Kodak 2	±8.32	±13.47	±4.51	±14.57
Kodak 3	--	±13.89	±6.85	±6.58
Gafchromic 1	±14.21	±17.85	±16.70	±9.93
Gafchromic 2	±10.85	±10.21	±10.78	±12.74
EPID 1	--	--	±6.32	±7.67
EPID 2	--	--	±5.88	±6.43

All the average leaf position values for CMJAH were below 96 % and thus on average the leaves were behind leaf 21 out of the field. The CMJAH deviation values were all greater than 10% for all imaging devices except for the leaf position accuracy test procedure results obtained with the Kodak film. Both these results were expected as seen in figure 6.4 where on average the leaf were below leaf 21 and there were leaves which had values in the range of 70 – 120%.

The average leaf position values for LH were above 100% before maintenance service on the Linac and below 100% after the service. This trend was seen with all the imaging devices except the Gafchromic film. The LH deviation values varied greatly with only the EPID values being below 10% constantly. Both these results were expected as seen in figure 6.5 where on average the leaves were below leaf 20 and there were leaves which have values in the range of 80 – 120%

The position with respect to leaf 21 for CMJAH and leaf 20 at LH is known but the distance that corresponds to these values is not yet quantifiable, even though the average leaf position results and the graphic representation of the leaf position as in figure 6.4 was known. The current method of leaf adjustment required the production of the graph as figure 6.4 to

determine which leaves had to be moved. The actual adjustment was conducted with visual display of the leaves position. Thus, further research is required for this analysis to produce a relationship between the percentage leaf deviation from 100% (leaf 21 at CMJAH and leaf 20 at LH) and physical distance of the leaves in mm.

6.4 Intraleaf Leakage Test Procedure Analysis

The intraleaf leakage data were analysed by imaging device as the dose calibration applied to each imaging device affects the resultant dose levels especially in the low dose range associated with scatter. Thus, the data obtained for each imaging device taken first at each institution namely LA 48 1, Kodak 1, Gafchromic 1 and EPID 1 (September 2014 for CMJAH and November 2014 for LH) were used as the baseline for that imaging devices data set as per the abuttal test procedure.

The expected result and therefore the baseline of the intraleaf test procedure will have a central spike and low percentage peaks at each leaf side as shown in figures 5.9, 5.22 and 5.23. The CMJAH intraleaf leakage was expected to be around 5 % of the maximum whereas the LH results were expected to be around 20 % due the back-up jaw not being present in the fields for the procedure.

The expected results for the combined test procedure will have no central spike as shown in figures 5.10(c) and 5.24(c). This was due to the difference in field design between the combine test procedure and the intraleaf test procedure. The readings were normalised to the reading at CAX and as this is not an open leaf dose the values obtained were due to scatter. Thus, these values were in the percentage range of 80 – 120% of CAX and not 5 – 20% seen in the intraleaf leakage test procedure results. There was also no expected percentage value for the combined test procedure results but the variation from the baseline data set must be within the tolerance shown in table 6.1.

Table 6.5: The average intraleaf transmission percentage for the intraleaf leakage test procedures at both CMJAH and LH for all imaging devices.

Imaging Device	CMJAH average intraleaf transmission (%)	LH average intraleaf transmission (%)
LA 48 1	3.81	--
LA 48 2	--	--
Kodak 1	3.30	12.21
Kodak 2	2.84	13.44
Kodak 3	0	7.49
Kodak 4	0	5.14
Gafchromic 1	9.67	19.53
Gafchromic 2	14.3	22.49
EPID 1	--	13.59
EPID 2	--	9.03

Table 6.6: The average intraleaf transmission percentage for the combined test procedures intraleaf leakage results at both CMJAH and LH for all imaging devices.

Imaging Device	CMJAH combined average intraleaf transmission (%)	LH combined average intraleaf transmission (%)
LA 48 1	83.45	--
LA 48 2	79.75	--
Kodak 1	86.36	94.33
Kodak 2	85.76	--
Kodak 3	84.39	94.42
Kodak 4		89.27
Gafchromic 1	111.45	124.48
Gafchromic 2	90.99	110.06
EPID 1	--	96.09
EPID 2	--	98.14

Due to the difference in field orientations used for the intraleaf leakage test procedure and the combined test procedure a direct comparison of the results is not possible. The results though should be consistent with each other.

The intraleaf leakage test procedure results for the Kodak 1 and LA 48 1 baseline values and subsequent values were within the expected value and the tolerance expressed. For the combined test procedure, the values differed from the baseline value within the expressed tolerances as well, except for the Gafchromic film.

All the imaging devices and procedure type had the same trend with the results of the later reading being lower than the earlier results. This was not observed with the intraleaf leakage test procedure results for the Gafchromic film (Gafchromic 1) at both CMJAH and LH.

6.5 Abuttal Test Procedure Analysis

The abuttal test procedure could only be conducted on the Siemens Linac at CMJAH as the Elekta MLC is unable to abut as discussed previously. The expected result of the abuttal procedure was a smooth continuous profile with no spikes. The expected results for the abuttal in the combined test procedure were different from the abuttal test procedure results. This was due to the open fields in the combined test procedure for the leaf position accuracy test procedure. Thus, a straight line result was not possible but as seen in figure 5.10(d), the slope from ± 50 mm should be a smooth curve.

Each imaging device would have its own baseline reading as the dose calibration of each imaging device was different. The dose calibration and the low dose range of the results would also result in the profiles not being continuously smooth.

6.6 Summary

The leaf matching, leaf position accuracy, leaf abuttal, intraleaf leakage and combined test procedures were successfully carried out and analysed using different detectors on two Linac systems at CMJAH and LH. Further investigation is required for the leaf matching and leaf position accuracy test procedures to produce comprehensive quantitative results. The validity of the imaging devices results can only be confirmed by physical comparison with the MLC and the subsequent MLC adjustment according to the results obtained per imaging device.

All the imaging devices produced differing values for each of the test procedures but all follow the same trends. Thus, an imaging device must be chosen which is most consistent in

response and in availability to the user. The Gafchromic film differed from the other imaging devices for all the test procedure either in result values or data trend. This was related to the low sensitivity of the Gafchromic film in the dose range evaluated.

7. RECOMMEDATIONS

The following was concluded from this thesis:

- The leaf matching, leaf position accuracy, leaf abuttal and intraleaf leakage test procedures evaluated in this thesis are the most relevant for the calibration and characterisation of an MLC system to current international standards and tolerances.
- A successful and reproducible QA program can be established from these procedures as currently being executed at CMJAH.
- The program can be successfully applied on different MLC configurations as at LH with equivalent effectiveness.
- A combined test procedure can replace the four individual procedures as a constancy check and does achieve results within the accepted tolerances of the individual procedures.
- A combined test procedure requires less execution time and also uses less material (i.e. film, processor).
- Further investigation is required into the methodology of the leaf matching test procedure to obtain complete quantitative analytical information on the MLC jaw symmetry and matching.
- Further research is required in the analysis of the leaf position accuracy test procedure in order to quantify the physical distance of the leaves from their ideal position.
- The various imaging devices produced consistent and comparable results within tolerance of each other except for the Gafchromic film, which has a low sensitivity in the low dose ranges used for these test procedures.
- The investigator recommends that the combined test procedure be conducted on all Linac MLC systems to establish a system baseline and then repeated at a frequency as stipulated in current international standards.
- The investigator strongly recommends that the radiographic Kodak film is used as the imaging device to record the results as it has consistently reproducibly results in the dose range investigated.
- If Kodak film is not a viable option for the department due to issues discussed, the investigator recommends that the LA 48 linear array is used as the imaging device as it has real time results and a high resolution is achievable.
- If neither the Kodak film nor the LA 48 linear array is available due to departmental resources the investigator recommends that the EPID system is used as the imaging device to record the results. The EPID systems are currently widely in use and available and has the shortest set-up, exposure, image retrieval time of all the imaging devices examined in this thesis.

- The investigator recommends that the test procedures be examined for the full photon energy range available on the Linac system as well as at major gantry positions.
- The investigator recommends that great caution should be taken in the commissioning of IMRT or other small field techniques as the baseline of the system set up within the required standards for the techniques must be well defined and evaluated to be able to determine the reproducibility and stability of the MLC over time for these techniques.
- The investigator recommends that the test procedures be examined using smaller volume ion chambers, 2D arrays and new imaging devices functioning in low dose small field dosimetry.

8. REFERENCES

1. F. M. Khan. **The physics of radiation therapy**, 4th edition. Lippincott Williams & Wilkins, 2010.
2. AAPM Radiation Therapy Committee. Task Group 50. **Basic applications of multileaf collimators**. American Association of Physicists in Medicine. 2001. [Online] Available from: <https://www.aapm.org/pubs/reports/> [Accessed December 2013]
3. C. Liu, T. A. Simon, C. Fox, J. Li, & J. R. Palta. Multileaf collimator characteristics and reliability requirements for IMRT Elekta system. **International Journal of Radiation Oncology Biology Physics**, 2008, **71** (1), p. S89-S92.
4. G. A. Ezzell, J. M. Galvin, D. Low, J. R. Palta, I. Rosen, M. B. Sharpe, **et al.** Guidance document on delivery, treatment planning, and clinical implementation of IMRT: Report of the IMRT subcommittee of the AAPM radiation therapy committee. **Medical Physics**, 2003. **30** (8), p.2089.
5. S. Webb. Volumetric-modulated arc therapy: its role in radiation therapy. **Medical Physics Web Article**. 2009, [Online] Available from: <http://medicalphysicsweb.org/cws/article/opinion/39542> [Accessed May 2016]
6. D. Wyman, P. Munro, **et al.** **Standards for Quality Control at Canadian Radiation Treatment Centres: Linear Accelerator**. 2005. Canadian Association of Provincial Cancer Agencies (CAPCA). [Online] Available from: <http://www.medphys.ca/media.php?mid=134> [Accessed December 2012].
7. G. J. Kutcher, L. Coia, M. Gillin, W. F. Hanson, S. Leibel, R. J. Morton, **et al.** Comprehensive QA for radiation oncology: report of AAPM radiation therapy committee Task Group 40. **Medical Physics**, 1994, **21**, p.581.
8. M. Evans, C. Araujo, P. Dickof, **et al.** **Standards for Quality Control at Canadian Radiation Treatment Centres: Multileaf Collimator**. 2006. Canadian Association of

Provincial Cancer Agencies. [Online] Available from:

<http://www.medphys.ca/media.php?mid=135> [Accessed December 2012]

9. E. E. Klein, J. Hanley, J. Bayouth, F. F. Yin, W. Simon, S. Dresser, **et al.** Task Group 142 report: quality assurance of medical accelerators. **Medical Physics**, 2009, **36** (9), p.4197.
10. C. Kirkby, E. Ghasroddashti, C. Angers, **et al.** Technical Quality Control Guidelines for Canadian Radiation Treatment Centres: Medical Linear Accelerators and Multileaf Collimators. **Canadian Partnership for Quality Radiotherapy**.2013, [Online] Available from: <https://www.medphys.ca/media.php?mid=3733> [Accessed December 2013]
11. T. J. LoSasso. IMRT delivery system QA. **Intensity-modulated radiation therapy: The State of Art**. American Association of Physicists in Medicine, 2003, pp. 561-93.
12. T. J.LoSasso. IMRT delivery performance with a Varian multileaf collimator. **International Journal of Radiation Oncology Biology Physics**, 2008, **71** (1), S85-S88.
13. M. Sastre-Padro, U. A. van der Heide and H. Welleweerd. An accurate calibration method of the multileaf collimator valid for conformal and intensity modulated radiation treatments. **Physics in Medicine and Biology**, 2004, **49** (12), p. 2631.
14. E. E. Klein, W. B. Harms, D. A. Low, V. Willcut and J. A. Purdy. Clinical implementation of a commercial multileaf collimator: Dosimetry, networking, simulation, and quality assurance. **International Journal of Radiation Oncology Biology Physics**, 1995, **33** (5), p. 1195-1208.
15. J. E. Bayouth. Siemens multileaf collimator characterization and quality assurance approaches for intensity-modulated radiotherapy. **International Journal of Radiation Oncology Biology Physics**, 2008, **71** (1), p. S93-S97.

16. T. J. Jordan and P. C. Williams. The design and performance characteristics of a multileaf collimator. **Physics of Medicine and Biology**, 1994, **39** (2), p. 231-251.
17. S. J. Baker, G. J. Budgell, and R. I. Mackay. Use of an amorphous silicon electronic portal imaging device for multileaf collimator quality control and calibration. **Physics in Medicine and Biology**, 2005, **50** (7), p 1377-1392
18. M. Pasquino, V. C. Borca, P. Catuzzo, F. Ozzello, S. Tofani. Transmission, penumbra and leaf positional accuracy in commissioning and quality assurance program of a multileaf collimator for step-and-shoot IMRT treatments. **Tumori**. 2006, **92** (6), p 511 - 516.
19. J. E. Bayouth, D. Wendt, S. M. Morrill. MLC quality assurance techniques for IMRT applications. **Medical Physics**. 2003, **30** (5), p 743-750.
20. J. Chang, C. H. Obcemea, J. Sillanpaa, J. Mechalakos, C. Burman. Use of EPID for leaf position accuracy QA of dynamic multi-leaf collimator (DMLC) treatment. **Medical Physics**. 2004, **31** (7), p 2091-2096.
21. J. M. Galvin, A. R. Smith, B. Lally. Characterization of a multileaf collimator system. **International Journal of Radiation Oncology Biology Physics**. 1993, **25** (2), p 181-192.
22. M. N. Graves, A. V. Thompson, M. K. Martel, D. L. McShan, B. A. Fraass. Calibration and quality assurance for rounded leaf-end MLC systems. **Medical Physics**. 2001, **28** (11), p 2227-2233.
23. A. R. Hounsell, T. J. Jordan. Quality control aspects of the Philips multileaf collimator. **Radiotherapy and Oncology**. 1997, **45** (3), p225-233
24. M. S. Huq, I. J. Das, T. Steinberg, J. M. Galvin. A dosimetric comparison of various multileaf collimators. **Physics in Medicine and Biology**. 2002, **47** (12), N159-N170
25. D. A. Low, J. W. Sohn, E. E. Klein, J. Markman, S. Mutic, J. F. Dempsey. Characterization of a commercial multileaf collimator used for intensity modulated radiation therapy. **Medical Physics**. 2001, **28** (5), p752-756

26. T. LoSasso, C. S. Chui, C. C. Ling. Physical and dosimetric aspects of a multileaf collimation system used in the dynamic mode for implementing intensity modulated radiotherapy. **Medical Physics**. 1998, **25** (10), p1919-1927
27. L. Parent, J. Seco, P. M. Evans, D. R. Dance. A. Fielding. Evaluation of two methods of predicting MLC leaf positions using EPID measurements. **Medical Physics**. 2006; **33** (9), p 3174-3182
28. D. A. Low, J. M. Moran, J. F. Dempsey, L. Dong, and M. Oldham. Dosimetry tools and techniques for IMRT. **Medical Physics**, 2011, **38** (3), p. 1313-1338.
29. G. Marinello. Overview on dosimetry for modern techniques using high energy X-rays. **In Proceeding of AAPM ISEP: training course on clinical dosimetry and quality assurance for advanced radiation therapy techniques**, Prague, Czech Republic, 16-20 Jun. 2008. [Online] Available from http://www.iaea.org/inis/collection/NCLCollectionStore/_Public/40/003/40003876.pdf [Accessed on 1 May 2014]
30. H. Bouchard, J. Seuntjens, S. Duane, Y. Kamio and H. Palmans. Detector dose response in megavoltage small photon beams. I. Theoretical concepts. **Medical Physics**. 2015, **42** (10), p 6033-6047
31. H. Bouchard, Y. Kamio, H. Palmans, J. Seuntjens and S. Duane. Detector dose response in megavoltage small photon beams. II. Pencil beam perturbation effects. **Medical Physics**. 2015, **42** (10), p 6048-6061.
32. S. Pai, I. J. Das, J. F. Dempsey, K. L. Lam, T. J. Losasso, A. J. Olch, J. R. Palta, L. E. Reinstein, D. Ritt and E. E. Wilcox. Task Group-69: Radiographic film for megavoltage beam dosimetry. **Medical Physics**, 2007, **34** (6), p 2228-2255
33. A. Niroomand-Rad, C. R. Blackwell, B. M. Coursey, K. P. Gall, J. M. Galvin, W. L. McLaughlin, et al. Radiochromic film dosimetry: recommendations of AAPM radiation therapy committee task group 55. **Medical Physics**, 1998, **25** (11), p 2093-2115.

APPENDIX

Similarity Summary Report

LinearAcceleratorMultileafCollimatorQualityControlMethod...

ORIGINALITY REPORT

4%

SIMILARITY INDEX

3%

INTERNET SOURCES

3%

PUBLICATIONS

1%

STUDENT PAPERS

PRIMARY SOURCES

1	aapm.org Internet Source	<1%
2	www.peipfi-komdasulsel.org Internet Source	<1%
3	dspace.thapar.edu:8080 Internet Source	<1%
4	www.docstoc.com Internet Source	<1%
5	Wulff, Jörg. "Clinical Dosimetry in Photon Radiotherapy – a Monte Carlo Based Investigation", Philipps-Universität Marburg, 2010. Publication	<1%
6	www.aapm.org Internet Source	<1%
7	marco.stanford.edu Internet Source	<1%
8	Medical Radiology, 2012. Publication	<1%
9	www.drct.com	